Annales Geophysicae (2001) 19: 495–519 © European Geophysical Society 2001

Annales Geophysicae

Structure of the auroral precipitation region in the dawn sector: relationship to convection reversal boundaries and field-aligned currents

Y. I. Feldstein[1], L. I. Gromova[1], J. Woch[2], I. Sandahl[3], L. Blomberg[4], G. Marklund[4], and C.-I. Meng[5]

[1]Institute of Terrestrial Magnetism, Ionosphere and Radio Waves Propagation, Moscow Region, Russia
[2]Max-Planck-Institut für Aeronomie, Katlenburg-Lindau, Germany
[3]Swedish Institute for Space Physics, Kiruna, Sweden
[4]Alfvén Laboratory, KTH, Stockholm, Sweden
[5]Applied Physics Laboratory, Laurel, Maryland, USA

Received: 16 March 1999 – Revised: 3 April 2001 – Accepted: 5 April 2001

Abstract. Simultaneous DMSP F7 and Viking satellite measurements of the dawnside high-latitude auroral energy electron and ion precipitation show that the region of the low and middle altitude auroral precipitation consists of three characteristic plasma regimes. The recommendation of the IAGA Working Group IIF/III4 at the IAGA Assembly in Boulder, July 1995 to decouple the nomenclature of ionospheric populations from magnetospheric population is used for their notation. The most equatorial regime is the Diffuse Auroral Zone (DAZ) of diffuse spatially unstructured precipitating electrons. It is generated by the plasma injection to the inner magnetosphere in the nightside and the subsequent drift plasma to the dawnside around the Earth. Precipitating particles have a hard spectrum with typical energies of electrons and ions of more than 3 keV. In the DAZ, the ion pitch-angle distribution is anisotropic, with the peak near 90°. The next part is the Auroral Oval (AO), a structured electron regime which closely resembles the poleward portion of the nightside auroral oval. The typical electron energy is several keV, and the ion energy is up to 10 keV. Ion distributions are predominantly isotropic. In some cases, this plasma regime may be absent in the prenoon sector. Poleward of the Auroral Oval, there is the Soft Small Scale Luminosity (SSSL) regime. It is caused by structured electron and ion precipitation with typical electron energy of about 0.3 keV and ion energy of about 1 keV. The connection of these low-altitude regimes with plasma domains of the distant magnetosphere is discussed. For mapping of the plasma regimes to the equatorial plane of the magnetosphere, the empirical model by Tsyganenko (1995) and the conceptual model by Alexeev et al. (1996) are used. The DAZ is mapped along the magnetic field lines to the Remnant Layer (RL), which is located in the outer radiation belt region; the zone of structured electrons and isotropic ion precipitation (AO) is mapped to the dawn periphery of the Central Plasma Sheet (CPS); the soft small scale structured precipitation (SSSL) is mapped to the outer magnetosphere close to the magnetopause, i.e. the Low Latitude Boundary Layer (LLBL). In the near-noon sector, earthward fluxes of soft electrons, which cause the Diffuse Red Aurora (DRA), are observed. The ion energies decrease with increasing latitude. The plasma spectra of the DRA regime are analogous to the spectra of the Plasma Mantle (PM). In the dawn sector, the large-scale field-aligned currents flow into the ionosphere at the SSSL latitudes (Region 1) and flow out at the AO or DAZ latitudes (Region 2). In the dawn and dusk sectors, the large-scale Region 1 and Region 2 FAC generation occurs in different plasma domains of the distant magnetosphere. The dawn and dusk FAC connection to the traditional Region 1 and Region 2 has only formal character, as FAC generating in various magnetospheric plasma domains integrate in the same region (Region 1 or Region 2). In the SSSL, there is anti-sunward convection; in the DAZ and the AO, there is the sunward convection. At PM latitudes, the convection is controlled by the azimuthal IMF component (B_y). It is suggested to extend the notation of the plasma pattern boundaries, as proposed by Newell et al. (1996), for the nightside sector of the auroral oval to the dawn sector.

Key words. Magnetospheric physics (current systems; magnetospheric configuration and dynamics; plasma convection)

Correspondence to: J. Woch (woch@linmpi.mpg.de)

1 Introduction

The high-latitude precipitation of plasma with auroral energies at upper atmosphere altitudes is closely connected with processes in the near Earth space and describes the large-scale plasma structure of the Earth's magnetosphere. The present view about the auroral precipitation pattern is based

on ground-based observations of different geophysical phenomena, as well as on *in situ* measurements by low-altitude polar-orbiting satellites. Auroral data take a crucial role in the investigation of the plasma precipitation. These data allow one to receive information on the global distribution and spectra of precipitating plasma fluxes at the upper atmosphere altitudes (Akasofu, 1976; Craven and Frank, 1991). There is a rather good correlation between plasma regimes at geocentric distances of some Earth radii (R_e) and plasma regimes in the upper atmosphere (Weiss et al., 1992; Yamamoto et al.,1993; Sandahl and Lindqvist, 1990). Mid-altitude satellite data, on which these results are based, are the transitional link to the distant plasma domain, about which the knowledge is based on *in situ* observations by spacecraft with very eccentric orbits (Frank, 1985; Nishida and Ogino,1997; Nishida et al., 1998).

Low-altitude satellites have been widely used for the identification of the plasma precipitation structure in the nightside (Winningham et al., 1975) and dayside (Newell and Meng, 1992, 1994a) sectors. According to Winningham et al. (1975), the nearmidnight electron precipitation pattern can be subdivided into the diffuse and discrete forms of electron precipitation. The diffuse precipitation is located equatorward of the discrete precipitation. It was tentatively identified as precipitation from the Central Plasma Sheet (CPS), whereas the discrete forms were proposed to be connected with the Boundary Plasma Sheet (BPS). According to Sandahl and Lindqvist (1990), CPS and BPS are overlapping.

Newell et al. (1996) and Feldstein and Galperin (1996) have suggested the identification of the characteristic boundaries of different plasma precipitation patterns based not only on the structural characteristics, but also on the physical properties of the observed electron and ion fluxes. This more detailed classification of the auroral regimes and their boundaries takes into account not only the structural features of plasma fluxes, but also their spectra, energy flux values and average energies of electrons and ions. The new classification reflects the present view about plasma regimes in the nightside Earth's magnetosphere, up to a geocentric distance of tens of R_e and its manifestation at the upper atmosphere altitudes (Galperin and Feldstein, 1996).

Newell et al. (1991a), Woch et al. (1994) and Woch and Lundin (1993 a,b) disseminated the traditional identification of the plasma pattern by Winningham et al. (1975) to the dawn sector. Their results are based on the electron and ion precipitation patterns, as imaged by DMSP and Viking satellites. In addition to the traditional CPS and BPS, a region identified as Low-Latitude Boundary Layer (LLBL) has been introduced. This region is located poleward of the BPS and is characterized by soft structured electron precipitation and soft intensive ion flux. The precipitation connected with the Plasma Mantle (PM) is located futher poleward in the dayside. For this latter region, a decrease of the energy and number flux with increasing latitude and very soft ion spectra are characteristic. In some studies which identified plasma pattern according to particle measurements, their connection with field-aligned currents (FACs) and convection directions has also been investigated. In the late dawn sector ($\sim$ 10 MLT), large-scale field-aligned currents flow into the ionosphere at LLBL latitudes, and they flow out at BPS latitudes. Poleward and equatorward boundaries of the LLBL coincide within 1° of geomagnetic latitude, with corresponding boundaries of the downward FAC (Region 1) by Iijima and Potemra (1978). The Convection Reversal Boundary (CRB), which separates regions of different convection directions, is located inside the LLBL, with antisunward (sunward) flow poleward (equatorward) of the CRB. Thus, the convection is sunward in the equatorial part of the LLBL. The PM region lies on anti-sunward convecting field lines (Newell et al., 1991b). Woch and Lundin (1993a) have shown that ion number densities in the LLBL region strongly correlate with the solar wind densities. The LLBL is observed during a time interval from 12 to 04 MLT and the probability for the existence of such pattern decreases from $\sim$ 0.9 near noon, to 0.0 at 0300 MLT.

It should be pointed out that by using the term LLBL, the authors did not intend to suggest that the ion and electron populations, which constitute the LLBL region, are the precipitating portion of a population existing in the near equatorial magnetospheric boundary layer. They may well be the populations produced by the processes in mid- or even high altitude portions of the magnetospheric boundary layer.

Nishida et al. (1992, 1993) used Akebono electric field and particle measurements to study electron and ion precipitation at dawn. For electrons, the existence of a sharp boundary, called the Transition Boundary (TRB), has been deduced. Equatorward of that boundary, electrons with $E > 1$ keV are precipitating and poleward of the TRB, only polar rain electrons with energy less than several hundred eV are observed. On the poleward side of the TRB (i.e. on presumably open magnetic field lines), ion patches were registered, known as 'Circumpolar Ion Precipitation' (CPIP). The CPIP existence is typical during times when the interplanetary magnetic field has a southward orientation ($B_z < 0$). The CPIP is located primarily on open magnetic field lines in the sunward convection region and, therefore, it is impossible to interprete them as projection of the LLBL to low altitudes (where the convection is observed to be anti-sunward). Sometimes CPIP is not seen in the dawn sector. Such cases are relatively infrequent but tend to be found in active intervals when Kp is high. The CPIP ions in their high latitude part have supposedly leaked from the boundary region of the plasma sheet or they have been generated in the distant neutral sheet.

The aim of this paper is:

1) to consider the dawn plasma regimes of the auroral precipitation and to extend notations of plasma regime boundaries, as suggested in Newell et al. (1996) and Feldstein and Galperin (1996) for the nightside sector to the dawn sector;

2) to connect plasma regimes with the large-scale distributions of the upward and downward field-aligned current systems and directions of the magnetospheric convection;

3) to associate low- and mid-altitude plasma regimes with their source populations in the distant magnetosphere by using new models of the magnetospheric magnetic field and

ionospheric precipitation pattern, derived from individual high-latitude spacecraft passes, as well as from statistical studies;

4) to use essentially simultaneous DMSP F7 and Viking satellite plasma observations to study MLT variations of the boundary locations and the existence of different plasma regimes.

2 Instrumentation and observations

2.1 Instrumentation

Viking and DMSP 7 observations were used for this study. The Viking plasma instrumentation consists of seven spectrometer units, which measured the directional electron flux over the energy range of 0.01–200 keV and ion flux over the range of 0.04–40 keV. A detailed description is given by Sandahl et al. (1985). The satellite has an orbit with a 13530-km apogee and a 817-km perigee at an inclination of 98.8°. The electric field experiment on Viking consists of six spherical probes extended on wire booms from the satellite (e.g. Block et al., 1987). Four of these booms are 40 m long and located in the plane perpendicular to the spin axis. These probes provide information about the two spin plane components of the electric field, one nearly parallel to the magnetic field (the component E_1) and the other perpendicular to $\boldsymbol{B}$ and directed nearly opposite to the satellite's velocity vector (the component E_2). The latter, which is used in this study, is typically the dominant electric field component in a plane perpendicular to $\boldsymbol{B}$. The Viking magnetic field experiment includes a fluxgate magnetometer system to record the 3 magnetic field components with sensors mounted on a 2 m boom (Potemra et al., 1987). The sampling rate is 53 vector samples per second. It has an automatic ranging capability from ± 1024 to ± 65536 nT since the magnetic field strength varied from approximately 1500 to 40000 nT throughout the orbit. B_N (B_E) is the northward (eastward) magnetic component. A background field IGRF-85 is subtracted from the observed components. Positive (negative) gradient of B_E represents a downward (upward) FAC, provided that a FAC system has a sheet structure extending in the azimuthal direction.

The DMSP F7 satellite measures fluxes of electrons and ions within the 0.032–30 keV energy range in 20 logarithmically placed steps (Hardy et al., 1984). One full electron and ion spectrum is obtained each second. The satellite is three-axis stabilized and the detector apertures always point toward local zenith. Only particles well inside the loss cone are observed at the latitudes of interest herein. The DMSP F7 satellite is in a sun-synchronous nearly circular polar orbit at about 835 km altitude in the late morning/pre-midnight local time meridian, with orbital inclination of 98.7°.

Three components of the magnetic field were measured by the fluxgate magnetometer (Rich et al., 1985) and represent the radial (B_x), the north-south (B_y) and the eastward-westward (B_z) magnetic components in a spacecraft field-aligned coordinate system. Therefore, in the same way as in the Viking B_E component, positive and negative gradients in B_z indicate the satellite crossing of downward and upward flowing FAC sheets, respectively.

2.2 Results of the observations for the separate cases

Instances of dawn passes of Viking, when simultaneous measurements of plasma, the electric and magnetic fields were obtained, and solar wind plasma parameters were available, have been analyzed. Furthermore, there were DMSP F7 measurements during the $\sim$ 100 min intervals of Viking high-latitude passes. There were 15 intervals selected primarily during the March – May 1986 period. Detail descriptions of two of such cases are presented below.

2.2.1 Example 1: 17 March 1986

Figure 1a shows the satellite's trajectories in the coordinate system of corrected geomagnetic latitude (Φ) and magnetic local time (MLT). The start and end time (in UT) of each high-latitude pass is also given. Every 2 min position of Viking and 2.5 min position of DMSP F7 are marked.

The satellite's passes have been mapped to the magnetosphere equatorial plane using the magnetic field model by Tsyganenko (1995). The projection points are marked by numbers. In Fig. 1b, the corresponding UT for DMSP F7 (every $\sim$ 2.5 minute) are presented on the right, and for Viking(every 5 minute), on the left. Not all the satellite's location pass points map to the equatorial plane and only those that map to this plane earthward of 60 R_e are presented in the figure. The magnetopause has been represented by the equatorial section of the rotation paraboloid at $X \geq -20R_e$; its geocentric distance to the subsolar point has been calculated according to Roelof and Sibeck (1993). At the distance of $X < -20R_e$, the magnetopause is presented as a cylinder with the cross section radius equal to the paraboloid cross section radius in the same magnetosphere section.

During the 1600–1800 UT interval, hourly average values of the Interplanetary Magnetic Field (IMF) components are -1.4 nT and 1.0 nT for B_y, 4.0 nT and 2.4 nT for B_z; hourly average values of the solar wind velocity V are 390 km/s and 394 km/s, and for density n, 17.5 cm^{-3} and 16.9 cm^{-3}. Values averaged over 5 min show that V and n hardly change, B_z decreases from 7 nT to 0 nT, remaining positive during the whole interval, and B_y is small and unstable, repeatedly changing sign. The observations fall into the final period of the recovery phase of a magnetospheric substorm (AU is 30 nT and 25 nT, AL is -67 nT and -24 nT, AE is 98 nT and 50 nT, Kp is 2$-$, and Dst is -14 nT and -11 nT).

The DMSP F7 particle spectrograms are shown in Fig. 2. Note that the ion energy scale is inverted, so that higher-energy ions are towards the bottom and that the color scale corresponds to the differential energy flux. The spectrograms have a rather complicated structure. Moving from equatorward on the poleward bound section, DMSP F7 intersected the dawn sector and then reached the nightside sector of the precipitation region before going into the polar cap. Fol-

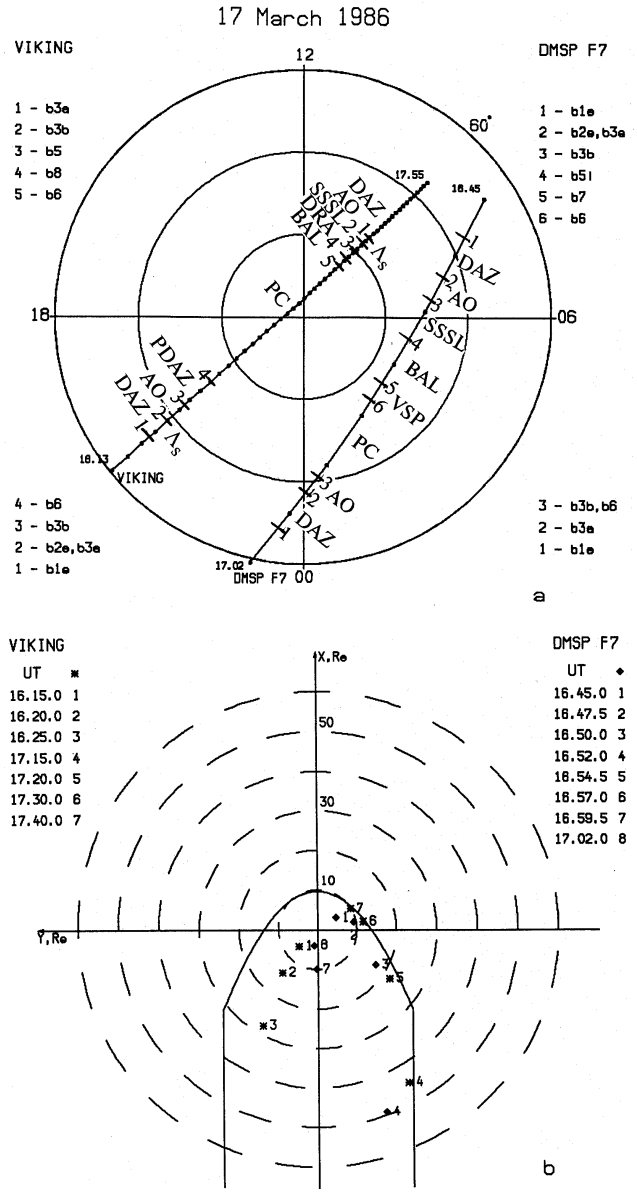

Fig. 1. **(a)** Trajectories of the Viking and DMSP satellites and plasma regimes in the high-latitude region of the northern hemisphere on 17 March 1986. Dots mark satellite positions every 2 min, and 2.5 min, respectively. Plasma regime boundaries are marked and their notations are presented for DMSP to the right, and for Viking, to the left; **(b)** projections of the trajectory points to the magnetospheric equatorial section, using the Tsyganenko (1995) model. Numbers are used to mark the UT moments for which the satellite's coordinates are shown in the spectrograms in Fig. 2 and Fig. 5. They identify the various boundaries, separately for the dawn and dusk part of the orbit.

lowing Newell et al. (1991) and Woch et al. (1994), it is necessary to subdivide the precipitation region in the dawn sector into 4 distinct regimes. However, for these regimes, a nomenclature is used which is decoupled from the magnetospheric populations, in contrast to the CPS, BPS, LLBL and PM notation used in the above mentioned papers. First, in the equatorward region, a diffuse precipitation is encountered; these electrons of high-energy have drifted from the nightside (DAZ – Diffuse Auroral Zone); the second region is indentified by the existence of softer and spatially sporadic electrons. Discrete auroral arcs and electron acceleration events are embedded within the soft background electron precipitation (AO – Auroral Oval); the next regime is characterized by softer electron precipitation. The electrons tend to be beam-like, with their average energy less than about 0.4 keV; the spectral peak in the ion flux is about 10^7 eV/(cm^2 s sr eV) (SSSL – Soft Small Scale Luminosity). Finally, further poleward, a precipitation is encountered with de-energized magnetosheath ions and usually, but not necessarily always, electron precipitation at the level of intense polar rain or higher. The particle's average energy is usually several tens of eV, up to about 200 eV (DRA – weak Diffuse Red Aurora). This diffuse red luminosity is encoutered with electron precipitation from the Plasma Mantle (PM) in the dawn sector and from the plasma sheet boundary portion (PDAZ) in the near midnight sector.

The nightside low-altitude plasma precipitation structure and its connection with the large-scale plasma structure of the distinct magnetosphere are, in detail, examined by Newell et al. (1996), Galperin and Feldstein, (1996), Feldstein and Galperin, (1996). Below, the identification of plasma regimes and their boundary notations, suggested in these papers, are used to interprete plasma observations by the DMSP F7 and Viking satellites. These notations fulfilled the recommendation of the IAGA Working Group IIF/III4 'Extention of the Auroral Oval and Polar Cap into the Magnetosphere' at the IAGA Assembly in Boulder, July 1995. This recommendation is as follows: 'The community should decouple nomenclature of ionospheric populations from magnetospheric population, creating a set of operation definitions which are model independent'. Below, the notations used for the nightside sector have been kept for the same type of plasma structures on the dawn sector, but new notations for new plasma regimes and boundaries between them are introduced.

Moving to high latitudes, DMSP F7 has registered for the first time an auroral plasma at 1646:53 UT at a latitude of $\Phi = 68.6°$ and a magnetic local time of 7.7 MLT ($b1$ boundary). The diffuse precipitation of electrons with energy up to $E \sim 10$ keV has been observed until 1647:52 UT ($\Phi = 71.0°$ at 7.3 MLT), where auroral energy ion precipitation was practically absent (DAZ). According to Fig. 1b, this maps into the outer radiation belt region, where electrons injected from the nightside plasma sheet have drifted to the dawnside and have also taken part in the convecting motion. Since the energy of the plasma which takes part in the convection is considerably less than the energy in the radiation belt, this region is called the Remnant Layer (RL), as it has been suggested in Feldstein and Galperin (1985).

At 1647:52 UT, the satellite intersects a boundary poleward where average electron energy begins to decrease, though the energy flux is kept at a high level of $\sim 8 \times 10^{11}$ eV/(cm^2 s sr). The electron precipitation be-

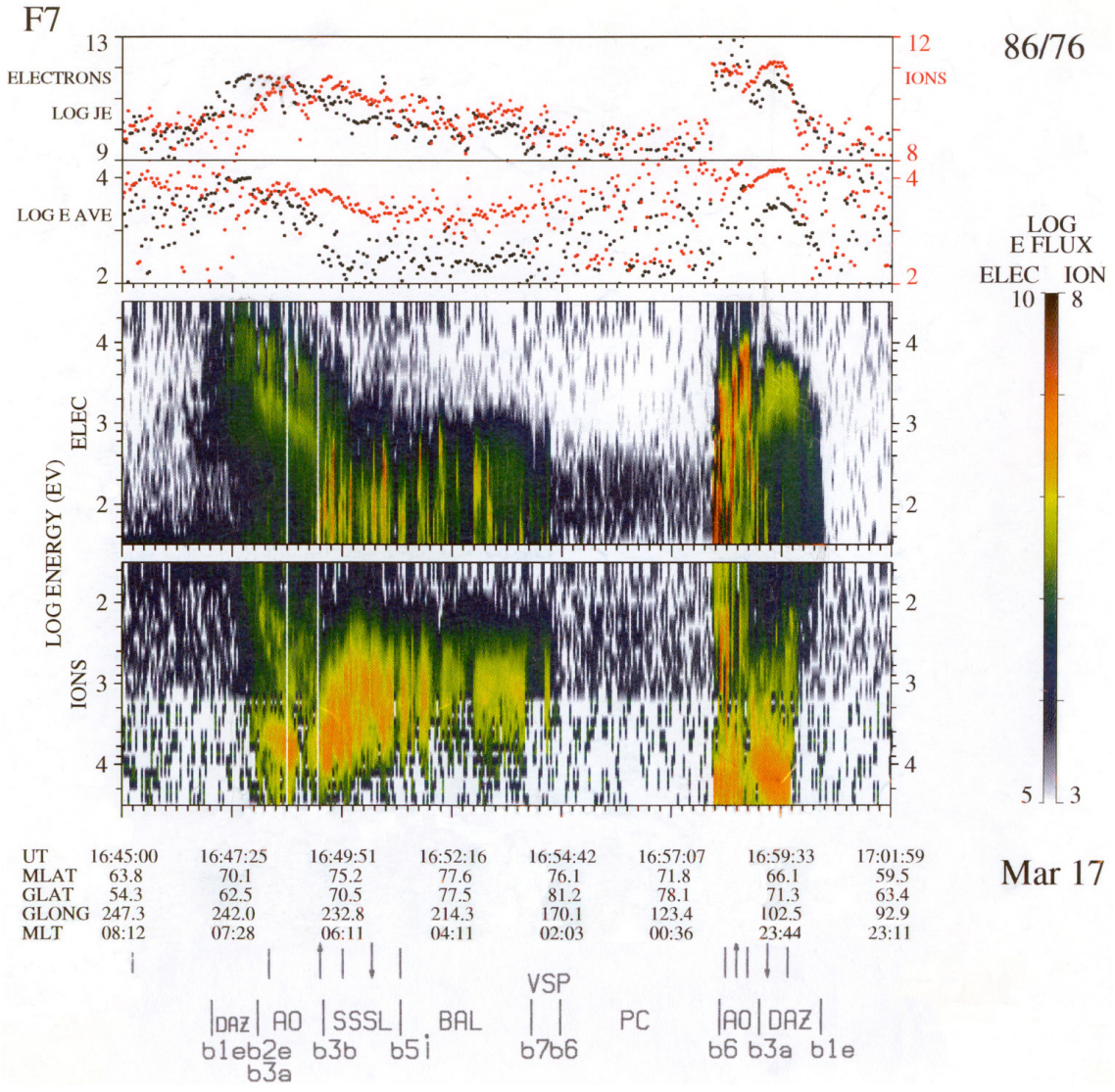

Fig. 2. DMSP F7 spectrograms of particle differential energy flux in units of eV $(cm^2\ s\ sr\ eV)^{-1}$ on 17 March 1986, 1645–1700 UT. Note that the ion energy scale is inverted. The line at the top plot is the integral energy flux eV $(cm^2\ s\ sr)^{-1}$, while the lower plot is of average energy (eV). The particle regime boundaries are marked, their notations are indicated; field-aligned current directions are marked by arrows.

comes structured and precipitating ions with energy from 0.1 keV to 20 keV appear. It is the poleward boundary of diffuse precipitation (*b*2*e*) and the beginning of the structured precipitation regime (AO) with its equatorward boundary *b*3*a*. The poleward boundary of this region *b*3*b* is crossed by the satellite at 1649:22 UT ($\Phi = 74.5°$ and 6.4 MLT), when the electron energy sharply decreases, the electron fluxes become extremely structured, and the average ion energies and energy fluxes begin to smoothly decrease with increasing latitude. The magnetosphere region, usually referred to as the Central Plasma Sheet (CPS), is mapped to the AO latitudes, i.e. between the *b*2*e* (*b*3*a*) and *b*3*b* boundaries.

The region of soft, small-scale precipitation luminosity (SSSL), associated by Newell et al. (1991) with the Low Latitude Boundary Layer (LLBL), is located poleward of *b*3*b*. Indeed, the mapping to the magnetospheric equatorial plane, using the model by Tsyganenko (1995) and Alexeev et al. (1996), shows that this part of the satellite pass maps to the region near the magnetospheric boundary (Fig. 1b). The LLBL poleward boundary, called as *b*5*i*, is marked by an interruption of the average ion energy and ion energy flux decrease. The boundary is intersected by the satellite at 1650:57 UT ($\Phi = 76.4°$ and 5.2 MLT). The soft electron flux (PDAZ – Polar Diffuse Auroral Zone) is observed up to 1654:28 UT ($\Phi = 76°$ and 2.2 MLT). At this boundary the polar rain begins (*b*6). This region of soft electron and ion precipitation is mapped along magnetic field lines deeply into the magnetospheric tail (Fig. 1b). According to its spectral peculiarities, it must be divided into 2 regions: in the first, there is structured and rather intensive electron and ion precipitation (BAL – Boundary Auroral Luminosity, its boundary is *b*7 at 1653:58 UT, $\Phi = 76.6°$ and 2.6 MLT); in the second,

there is diffuse and very soft electron and ion precipitation (VSP – Very Soft Precipitations). These two structures are mapped to the Plasma Sheet Boundary Layer (PSBL) (the region between $b5i$ and $b7$) and the Low Energetic Layer (LEL) (the region between $b7$ and $b6$). Such a complicate character of the particle spectrogram is caused either by the satellite crossing more plasma sheet domains in the nightside magnetosphere before entering into the polar rain regime, or by temporal fluctuations.

The polar rain precipitation characterizes the Polar Cap (PC) plasma (outside $b6$ boundary). From this region, the satellite intersects in the near midnight sector at 1657:59 UT ($\Phi = 70°$ and 0.2 MLT) first the $b6$ ($b3b$) boundary and then sequentially the boundaries $b3a$ (1658:50 UT, $\Phi = 67.5°$, 00 MLT), and $b1e$ (1700:25 UT, $\Phi = 63.8°$, 23.5 MLT). The regions between them correspond to the AO and DAZ regimes, which correspondingly map to the CPS and RL magnetospheric plasma domains in the nightside magnetosphere.

Figures 3a–f show samples of the precipitating electron and ion spectra in the different plasma regimes. The spectra presented in Fig. 3 are typical for their regimes. For dawn-night traversals, it can be seen from Fig. 3:

1) between the $b1e$ and $b2e$ ($b3a$) boundaries, there are rather large fluxes of electrons with E of several keV, and there are practically no auroral energy ions (Fig. 3a);

2) between the $b2e$ ($b3a$) and $b3b$ boundaries there are characteric electron spectra with peaks near 10 keV, and precipitation of energetic ions with E up to several ten keV (Fig. 3b) is observed;

3) between the $b3b$ and $b5i$ boundaries electron energy fluxes reach up to 10^9 eV/(cm^2 s sr eV) with characteristic energy of $E \sim 10^2$ eV; ions have characteristic energy of several keV and energy flux of about 6×10^6 eV/(cm^2 s sr eV) (Fig. 3c). Such electron and ion spectra are typical for the LLBL – type of plasma observed at low altitudes by the DMSP satellites;

4) between the $b7$ and $b6$ boundaries precipitation of very soft electrons and ions is observed with particle flux lower (by some orders of magnitude) than in the other regimes (Fig. 3d).

For the night crossing after exiting from the polar cap, it has been established that:

1) between the $b3b$ and $b3a$ boundaries, the electron energy flux peaks at about 8×10^8 eV/(cm^2 s sr eV) with energy of several keV, and ion energy flux peaks at about 5×10^5 eV/(cm^2 s sr eV) in a wide energy range (Fig. 3e);

2) between the $b3a$ and $b1e$ boundaries, there are energetic electron and ion fluxes (Fig. 3f). One can see considerable differences in the ion spectra between the $b1e$ and $b3a$ boundaries in the dawn and nightside sectors. In the first case there are practically no ion fluxes of auroral energies, but ion fluxes reach appreciable values in the near-midnight sector.

Figure 4 shows the east-west component of the DMSP F7 magnetic field data corresponding to the pass in Fig. 2; the particle and current regimes are marked above the magnetograms. In the dawn sector, there is a good correspondence between the AO and upward FAC, as well as between

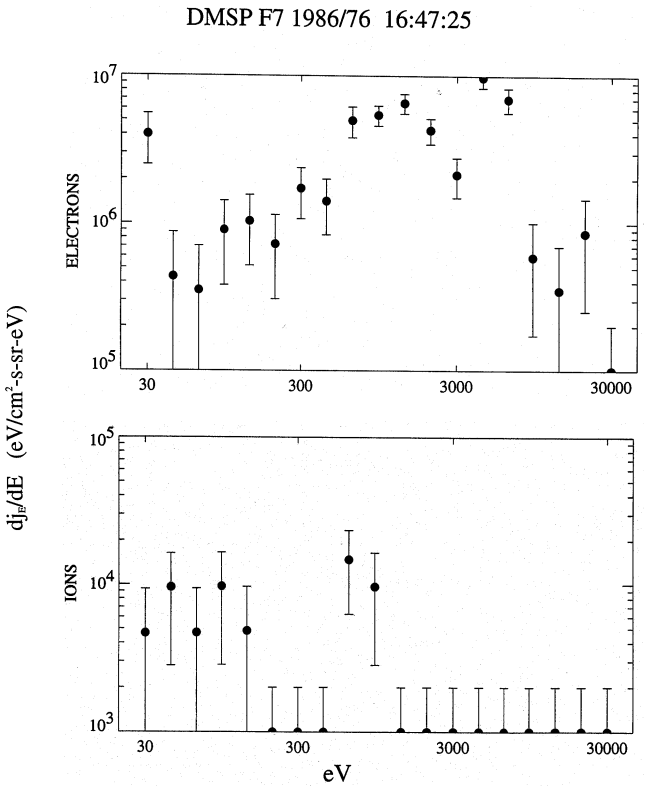

(a)

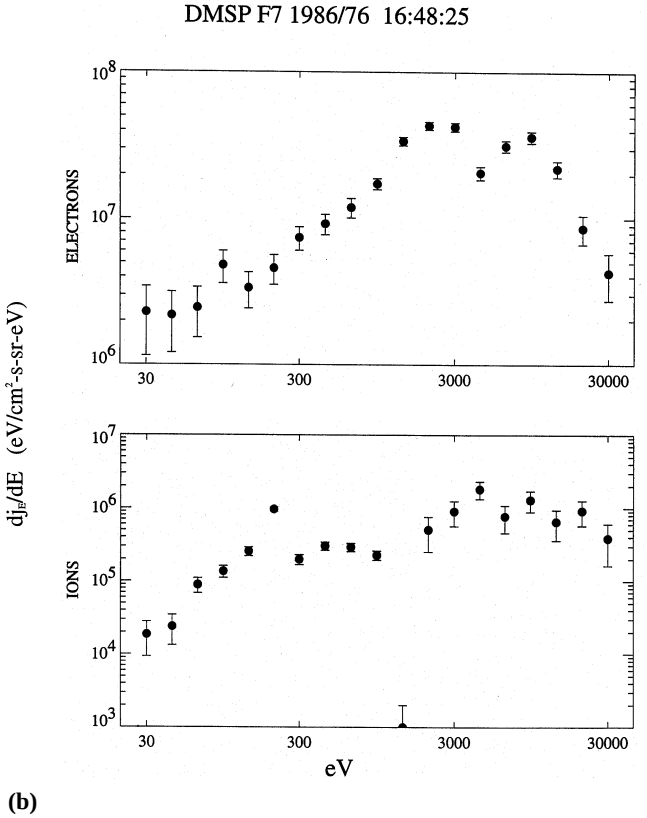

(b)

Fig. 3a-b. Electron and ion spectra observed at low altitude by DMSP F7 for the pass shown in Fig. 1. Plotted is the differential energy flux (circles with error bars) for various plasma regimes: **(a)** DAZ; **(b)** AO.

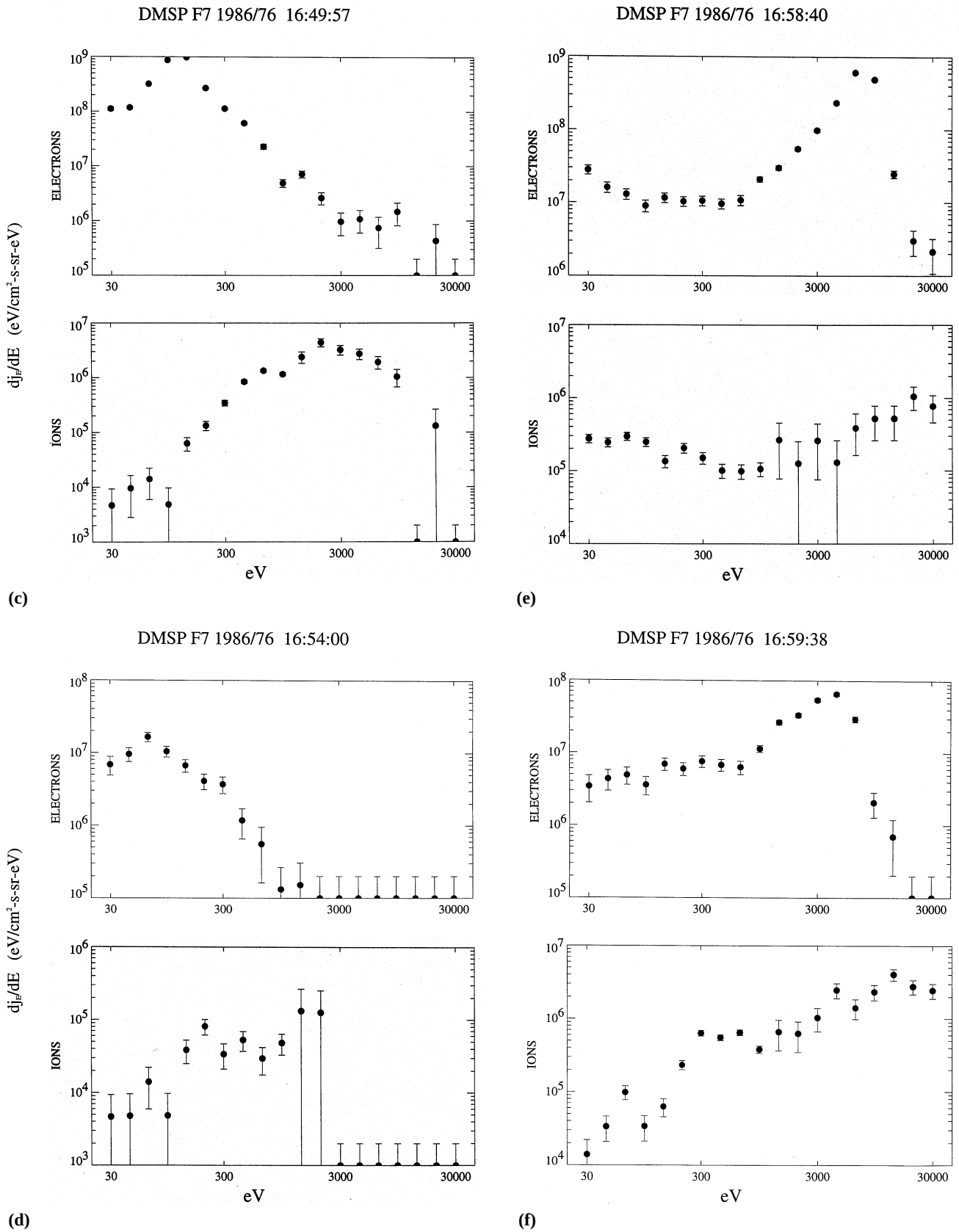

Fig. 3c-f. Electron and ion spectra observed at low altitude by DMSP F7 for the pass shown in Fig. 1. Plotted is the differential energy flux (circles with error bars) for various plasma regimes: **(c)** SSSL; **(d)** VSP; **(e)** AO; **(f)** DAZ.

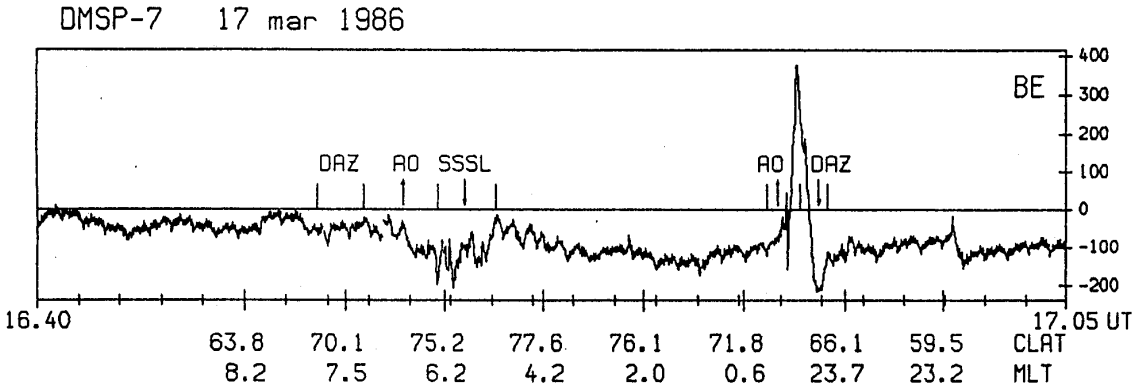

Fig. 4. The east-west component of the DMSP F7 magnetometer observations for the pass shown in Fig. 1. The particle regimes are marked above the magnetogram, the directions of the field-aligned current are marked by arrows. A positive gradient corresponds to a current flowing into the ionosphere.

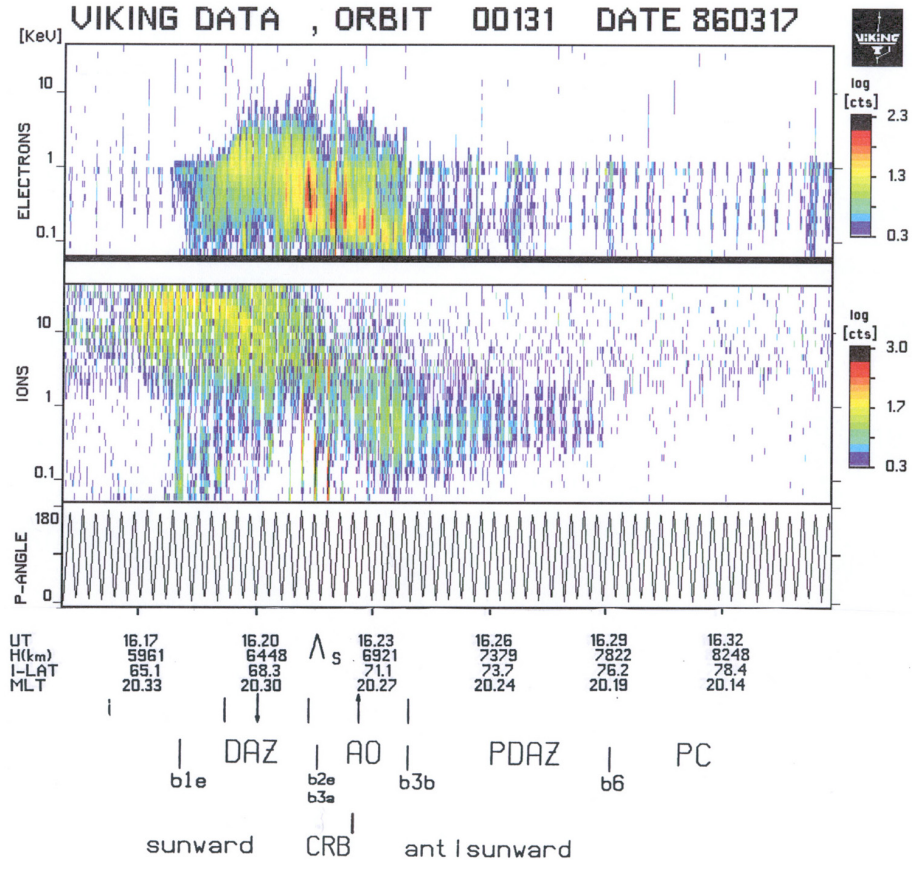

Fig. 5a. Viking particle spectrogram for orbit 131 on 17 March 1986, 1616–1727 UT. The plasma regimes and their boundaries, the convection reversal boundary (CRB) and field-aligned currents marked by arrows are given at the bottom: **(a)** the duskside sector.

the SSSL and downward FAC. This result is consistent with Newell et al. (1991a). In the near-midnight sector, there is a FAC system which consists of two sheets: a current outflow from the ionosphere in the high-latitude part of the auroral region, and an inflow to the ionosphere in the equatorward part.

On 17 March 1986 at 1613–1755 UT, the Viking satellite intersected the auroral region from evening to pre-noon, practically through the polar cap center (Fig. 1a). In Fig. 5a,b particle spectrograms observed during Viking orbit 131 are presented. At the bottom of the particle spectrograms, various particle precipitation regimes are outlined. The notations used for distinguishing the various mid-altitude plasma precipitation regions are the same as for the low-altitude

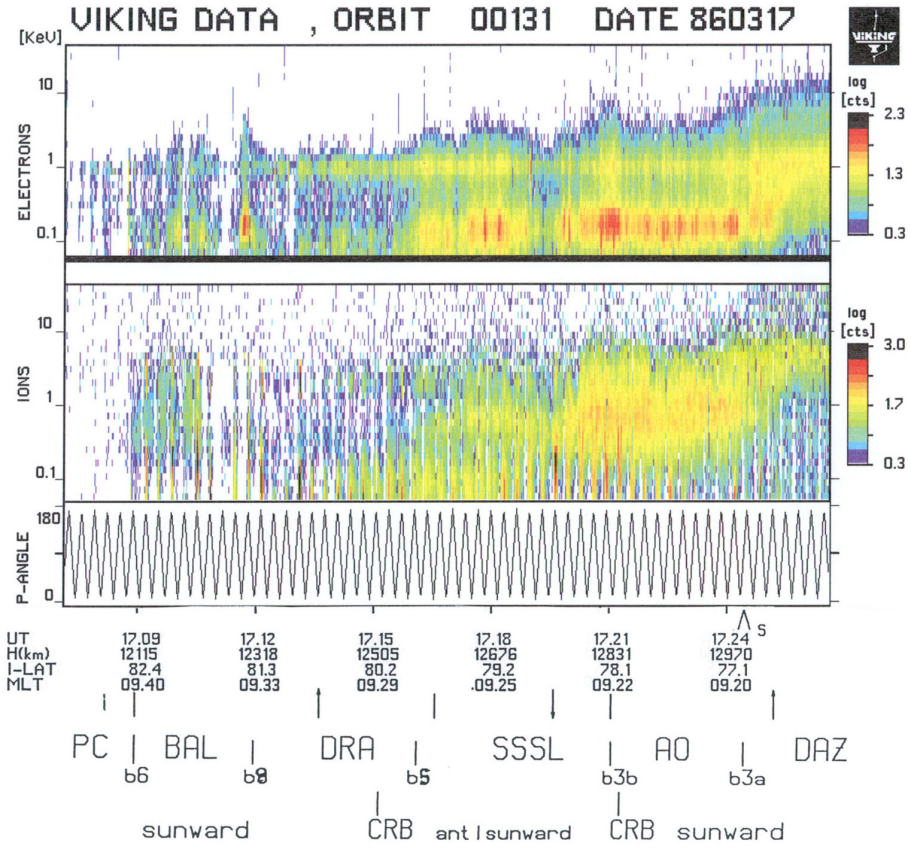

Fig. 5b. Viking particle spectrogram for orbit 131 on 17 March 1986, 1616–1727 UT. The plasma regimes and their boundaries, the convection reversal boundary (CRB) and field-aligned currents marked by arrows are given at the bottom: **(b)** the prenoon sector.

DMSP F7 satellite. The electron fluxes from 10 eV to 40 keV are presented in the top panel and the ion fluxes from 40 eV up to 40 keV, are presented in the second panel. Panel 3 shows the pitch-angle variation. Until 1618 UT, in Fig. 5a (the *b*1 boundary at $\Phi = 66.3°$ and 20.5 MLT), there is no auroral plasma precipitation seen, however trapped energetic ions are present. Till 1621 UT, the pitch-angle distribution expands and becomes more isotropic. The electron energy increases with latitude to several keV. At 1621 UT, the satellite crosses the boundary of stable electron trapping (Λ_s) with $E = 37$ keV. Poleward of the Λ_s, there are practically no electrons of such energies. Λ_s coincides with the boundaries of the monotonous electron energy growth, with latitude (*b*2*e*), and it coincides with the appearance of strongly structured electron fluxes (*b*3*a*) and upflowing ion beams. This boundary ($\Phi = 69.7°$ and 20.5 MLT) separates the DAZ from the AO. At middle altitudes, similar to low altitudes in the DAZ, there is precipitation of soft diffuse electrons and energetic ions; at the AO, structured electron precipitation and upflowing ion beams, with energies up to 1 keV, are observed. Simultaneously with increasing latitude, the electron and ion energies decrease. Apparently, when Viking was located at an altitude near 7000 km, it was well inside the plasma acceleration region as it is evident from electrons accelerating towards Earth and upward accelerated ions.

The AO high-latitude boundary *b*3*b* is crossed by the satellite at 1624 UT ($\Phi = 72.1°$ and 20.4 MLT). Poleward of this, there is the PDAZ, with soft and low-intensity plasma. The poleward boundary of this regime, which is the evening polar cap boundary, is crossed by the satellite at 1629 UT (*b*6, $\Phi = 76.2°$ and 20.4 MLT). Then the satellite enters into a region where only polar rain is observed. In the interval between *b*3*b* and *b*6, low-energy diffuse ion precipitation with isotropic distribution in the upper hemisphere is seen. According to their structure and location poleward of the AO boundary, this precipitation resembles the CPIP by Nishida et al. (1992).

At 1709 UT ($\Phi = 82.4°$ and 09.7 MLT), Viking intersects boundary *b*6 and the satellite enters into a region where there are obvious plasma acceleration processes (upflowing ion beams) and structural electrons precipitation (Fig. 5b). This region is mapped along the magnetic field lines to the magnetospheric tail and the satellite crosses a region, which is referred to as the BAL, with its equatorward boundary *b*8 (1712 UT, $\Phi = 81.3°$ and 9.5 MLT).

The regime DRA (Diffuse Red Aurora), in which there are very soft upflowing ion fluxes and soft diffuse electron fluxes, is adjacent to the PDAZ. The ion energies increase with decreasing latitude. Such spectra are typical for the plasma mantle (PM). In this way, the boundary *b*8 seperates

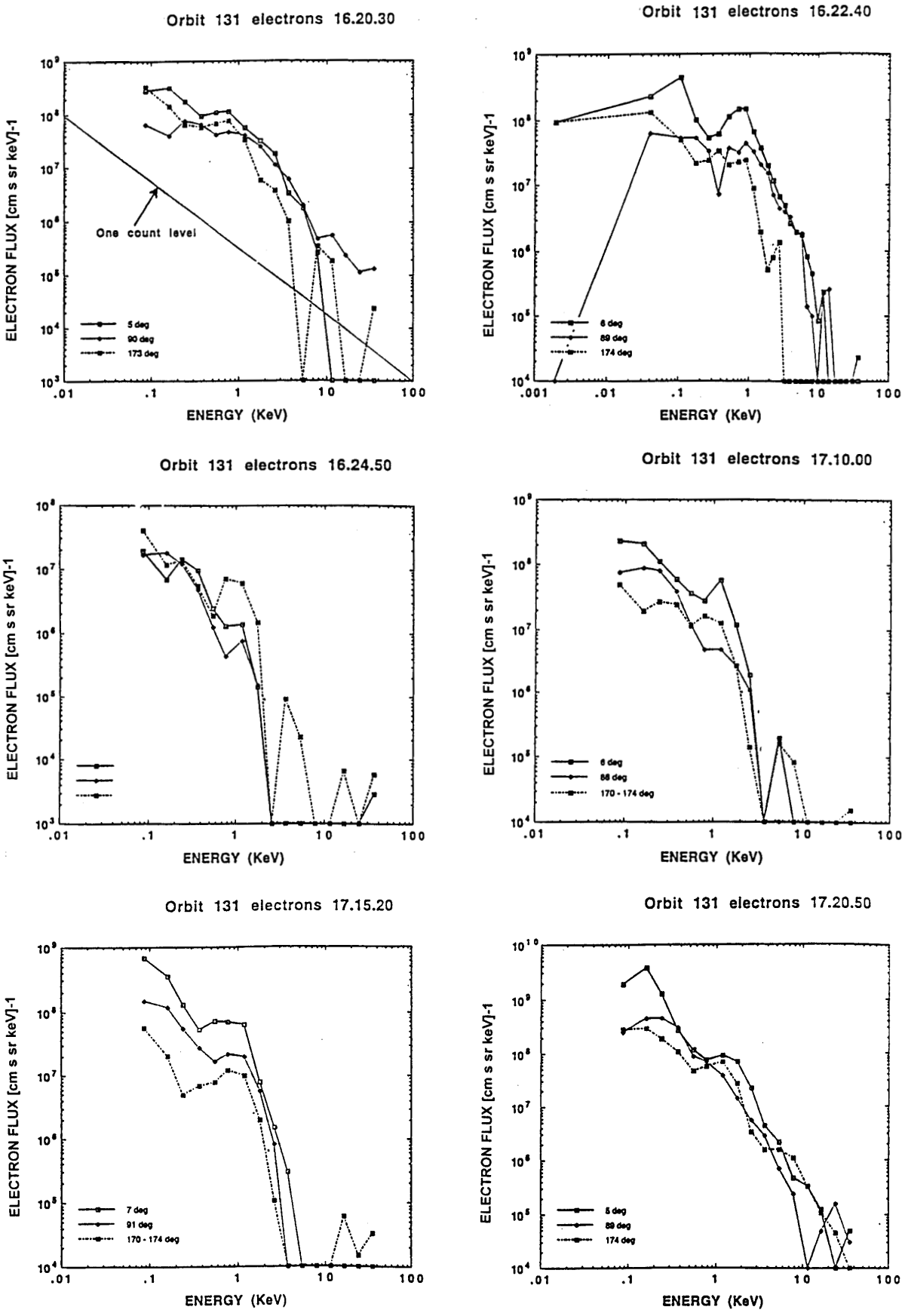

Fig. 6a. Electron spectra for different pitch-angles observed at mid-altitude by Viking on the pass shown in Fig. 5. The spectra were measured close to 0°, 90° and 180°.

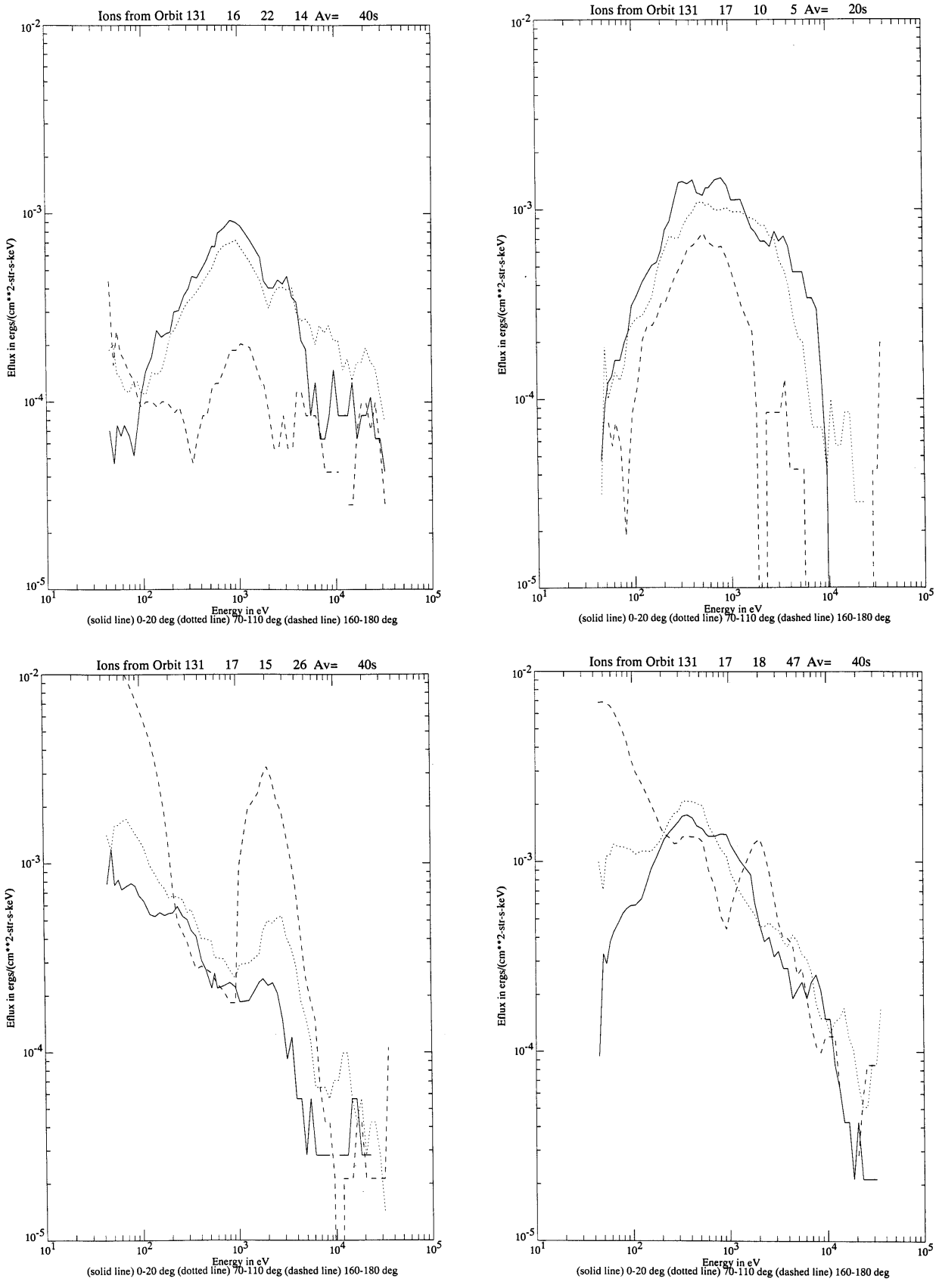

Fig. 6b. Ion spectra for different pitch-angles observed at mid-altitude by Viking on the pass shown in Fig. 5. The spectra were measured close to 0°, 90° and 180°.

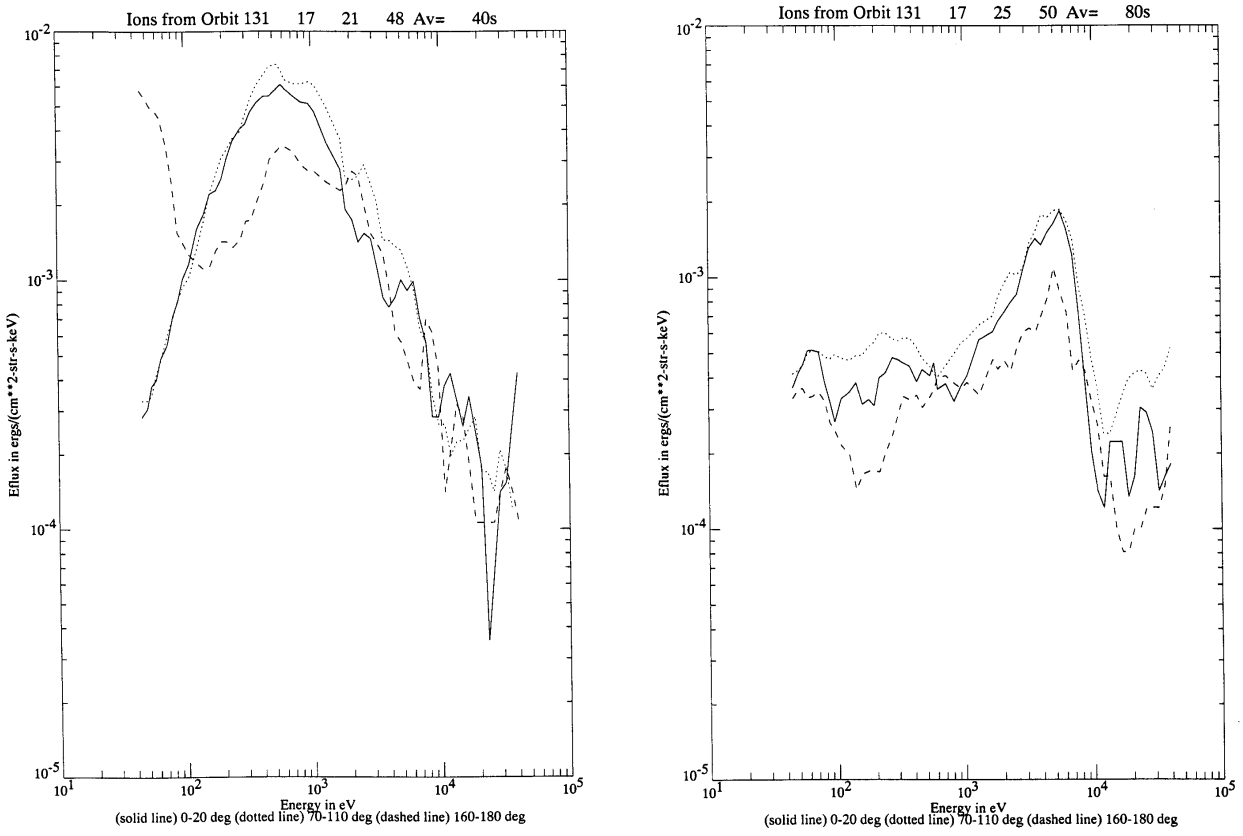

Fig. 6b. Continued.

PDAZ from DRA. The equatorward DRA boundary is $b5$ (1716 UT, $\Phi = 80°$ and 9.5 MLT). Then the satellite crosses the region of structured electron and ion fluxes, with very intensive upflowing ion beams, with energies less than 1 keV. Here, the average electron energies are somewhat higher than in the DRA regime. It is the Soft Small Scale Luminosity Regime (SSSL). So the boundary $b5$ separates the DRA from the SSSL. The equatorward SSSL boundary $b3b$ (1721 UT, $\Phi = 78.1°$ and 9.5 MLT) is also the AO poleward boundary. The boundary $b5$ is mapped along the magnetic field lines to the region close to the magnetospheric boundary (the magnetopause in Fig. 1b). Between 1721 UT and 1724 UT, the ion fluxes become isotropic at energies from 1 up to 10 keV; ion beams appear at energies up to several hundred eV. As the electron energies increase, their fluxes become more structured. It is the central plasma sheet which is extended towards the late dawn sector (AO), with its equatorward boundary $b3a$ (1724 UT, $\Phi = 77.1°$ and 9.3 MLT). Then the satellite enters into the regime DAZ with energetic electrons and ions, but without ion beams. The $b3a$ boundary coincides with the sharp increase of the 37 keV electrons flux, i.e. with the Λ_s.

In Fig. 6 electron (a) and ion (b) spectra for different plasma regimes are shown. The spectra are presented for three different pitch-angles, namely covering the loss cone (downward moving particles), perpendicular to the magnetic field line (trapped particles) and reflected (upward moving particles). The full pitch-angle distribution is measured in about 10 s, i.e. in half of a satellite spin.

At 1620:30 UT, downward moving electrons predominate at small energies (up to 1 keV), trapped electrons predominate at energies from 4 keV up to 20 keV and monotonously decreasing electron spectra, with electron flux $\sim 4 \times 10^8$ $(\text{cm}^2\ \text{s sr keV})^{-1}$ predominate at energies $\sim$0.1 keV. Precipitating particles with energies of more than 10 keV are virtually absent and the flux of trapped particles with $E \sim$ 20–30 keV is about 10^5 $(\text{cm}^2\ \text{s sr keV})^{-1}$. The ion flux is two or more orders less than the electron flux, there are no upward moving ions, and in the upper hemisphere, primarily isotropic distribution of ions with energy from 1 to 20 keV are measured (they are not shown in the figure). Such spectra are typical for plasma at auroral energies in the DAZ regime, which maps to the Outer Radiation Belt (Remnant Layer).

The characteristic electron and ion spectra for the discrete auroral forms are presented by spectra taken at 1622:40 UT for electrons, and at 1622:14 UT for ions. A secondary maximum for electrons appears at higher energies; the precipitating particles dominate, and trapped electrons with energies of $E > 20$ keV disappear. The ion fluxes are isotropic in the upper hemisphere with the maximum energy flux at 1 keV. All of these features are typical for the particle fluxes in the AO regime, which maps to the Central Plasma Sheet (CPS).

The electron spectrum near the auroral oval boundary in the PDAZ regime of the pre-midnight sector (spectra at 1624:50 UT) is a very soft spectrum. There are no electrons with $E > 3$ keV and the flux of electrons with $E \sim 0.1$ keV decreases practically by one order. The intensity of the upward moving particles is approximately the same as the intensity of the downward moving particles.

The spectra taken at 1710:00 UT are characteristic for the prenoon sector, adjacent to the polar cap boundary. In this sector, structured electron precipitation and intensive ion beams, typical for a region with plasma acceleration, have been measured by Viking. The precipitation of electrons with energy up to $E \sim 1.3$ keV dominates, with their fluxes sharply increasing at lower energies. Ion energy fluxes increase up to $\sim 2 \times 10^{-3}$ ergs/(cm^2 s sr keV) at energies of about 300 eV. In the loss cone the energy flux of ions has a maximum at energies of 300 to 800 eV. Although this region is located in the dawn sector at the polar cap boundary, it is mapped along the magnetic field lines to the nightside of the magnetosphere equatorial plane, deeply into the tail. However, apart from its ion spectrum, it is impossible to refer to it as DRA regime. It is located between the boundaries *b*6 and *b*8 (Fig. 5b) and it is natural to refer to it as PDAZ in the magnetosphere night sector.

Energy spectra typical for the region between boundaries *b*8 and *b*5 (the DRA poleward and equatorward boundaries) are the ones taken at 1715:20 UT. The spectral differences (especially ion spectra differences) give additional reasons to divide the poleward portion of the precipitation into two regimes between the boundaries *b*6–*b*8 and *b*8–*b*5. Fluxes of soft particles, upward moving ions and downward moving electrons predominate in the DRA. The ion spectra are very soft, and are typical for the region that Newell et al. (1991a,b) identified with the Plasma Mantle regime, which resides on open magnetic field lines.

The ion and electron spectra between boundaries *b*5 and *b*3*b* are essentially different from the spectra in the DRA (spectra around 1720 UT). In the electron spectra, the downward flux increases at times up to 4×10^9 (cm^2 s sr keV)$^{-1}$ for energy $E \sim 0.1$ keV and the upward flux increases by one order. The electron fluxes become quasi-isotropic, and the spectra are harder. Fluxes of particles with $E \sim 10$ keV appear. In the DRA regime, the ion energy fluxes for all pitch-angles decrease with energy increasing. Between boundaries *b*5 and *b*3*b*, the quasi monotonous decrease is only seen for the pitch-angles of about 180°. For particles with pitch-angles of about 0° and 90°, the energy spectrum is bell-shaped with the maximum at an energy of about 300 eV and an energy flux of about $\sim 2 \times 10^{-3}$ ergs/(cm^2 s sr keV). Such ion spectral character has been identified by Newell et al. (1991a) as the plasma precipitations from the LLBL (the SSSL regime). The ion spectra taken around 1722 UT characterize the AO regime. The energy flux of precipitating ions increases by an order of magnitude of $\sim 6 \times 10^{-2}$ ergs/(cm^2 s sr keV) at the maximum of the distribution located at 600 eV. Furthermore, there is a substantial increase in the energy flux in the hard part of the spectrum. Since the spectrum at 1722 UT is very different from spectra at 1719 UT and 1726 UT, we have to separate this regiom from the poleward and equatorward regions.

The last plasma regime equatorward of the boundary *b*3*a* is also shown in Fig. 6 (spectra around 1726). There, the fluxes of soft electrons with $E < 1$ keV decrease, the fluxes of electrons with $E > 20$ keV increase, and the population with pitch-angles of about 90° dominate. In comparison to the AO region, ion energy flux sharply decreases and the maximum of the flux is shifted to higher energies. This is the DAZ regime which maps along magnetic field lines to the outer radiation belt, where the motion of auroral energy plasma from the plasma sheet of the magnetospheric tail is dominated by the convection and injection connected with active processes in the nightside magnetosphere. This magnetosphere region was described as a reservoir for energetic particles ($E > 30$ keV) trapped by the geomagnetic field and has been called the Outer Radiation Belt (ORB). Yet in the same region, there are more intensive fluxes of electrons and ions with energies $E < 10$ keV, so that the integral plasma energy flux is many orders higher than the energy flux of the more energetic particles of the radiation belt. Feldstein and Galperin (1985) have suggested the identification of this magnetosphere region with auroral radiation as the Remnant Layer (RL). Although spatially the DAZ is mapped to the outer radiation belt region, the energy of the particle populations and their motion are completely different in ORB and RL. Therefore, in order to avoid any misunderstandings, the traditional notation for this region 'outer radiation belt' was not kept by Feldstein and Galperin, (1985). Another notation that is more closely corresponding to the origin of auroral energy particles in the inner magnetosphere have been introduced (remnants of the plasma sheet plasma, entering into the inner magnetosphere from the tail plasma sheet).

The location and direction of large-scale field-aligned currents flowing between the magnetosphere and the ionosphere can be obtained from the observation of the geomagnetic field variations by satellites crossing the high-latitude region (Zmuda and Armstrong, 1974). These currents, as a rule, are patterns sufficiently narrow in latitude (some degrees), but extending in longitude over some considerable distance. In Fig. 7, the variations of the east-west geomagnetic field component and the E2 component of the electric field measured by the Viking satellite in the dusk (Fig. 7a) and prenoon (Fig. 7b) sectors of the high-latitudinal region are shown. The east-west component is the most susceptible to longitudinally extended current layers. Despite the uncertainties of the electric field measurements, a reliable estimation of the predominant convection direction (sunward - antisunward) is possible throughout the region of interest. In Fig. 7, the FAC's directions are marked by arrows. The downward arrows mark currents flowing into the ionosphere, and the upward arrows mark outflowing currents. In the duskside FAC pairs are measured, with the inflowing current at 1620–1621 UT and the outflowing at 1621–1623 UT. In Fig. 7 the current direction is determined by the magnetic field gradient. A positive gradient is indicative for FAC flowing into the ionosphere,

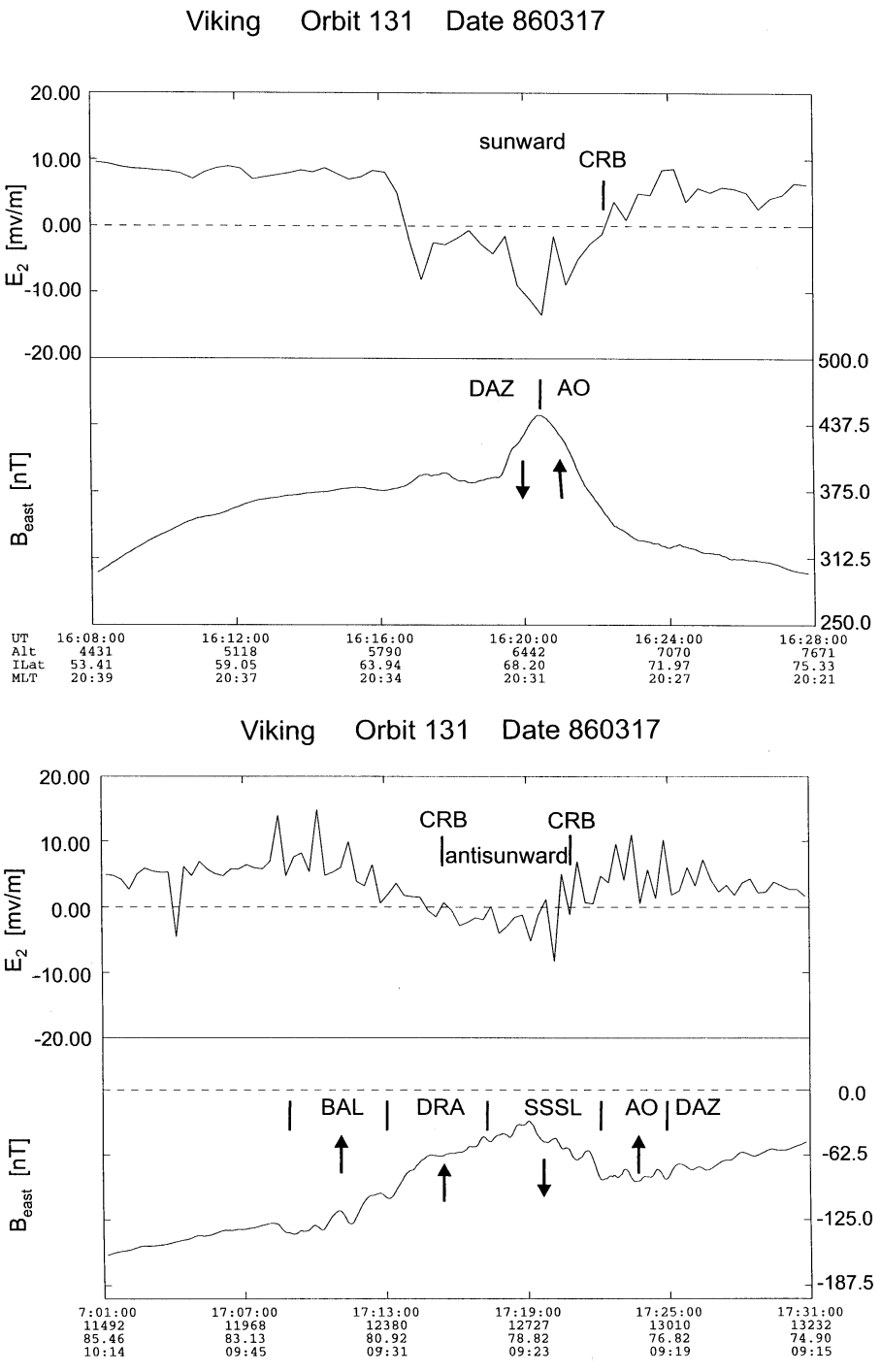

Fig. 7. The east-west component of the Viking magnetometer observations (bottom) and the spin plane component of the electric field (the component along the spaccraft trajectory, top) for the pass shown in Fig. 1: **(a)** the evening sector, **(b)** the pre-noon sector. The plasma regimes intersected by the satellite and directions of the FACs are marked at the top.

and a negative gradient indicates FAC flowing out from the ionosphere. The FAC direction agrees well with the patterns formly established at the early stage of auroral research. In the dusk sector, the currents flow into the ionosphere at the diffuse luminosity (precipitations) latitudes. Outflows occur at latitudes of the auroral discrete forms (structural precipitations) (Kamide and Akasofu, 1976). The boundary between FACs of different directions coincide with the plasma boundary *b*2*e* (*b*3*a*), separating the DAZ and the AO. The upward (downward) FACs coincide with Region 1 (Region 2) of the FAC by Iijima and Potemra (1978). Both upward and downward FACs are located in the sunward convection region equatorward of the CRB. In the prenoon sector, the magnetometer measures a more complicated FAC pattern (Fig. 7b): the field-aligned currents flow out from the ionosphere at 1709–1719 UT and after 1722 UT, and flow into the ionosphere at 1719–1722 UT. Such a three-layered FAC pattern is typical for the prenoon sector (Newell et al., 1991a), in such a way that the currents flow into the ionosphere in the SSSL regime (Region 1) and flow out at the AO–DAZ

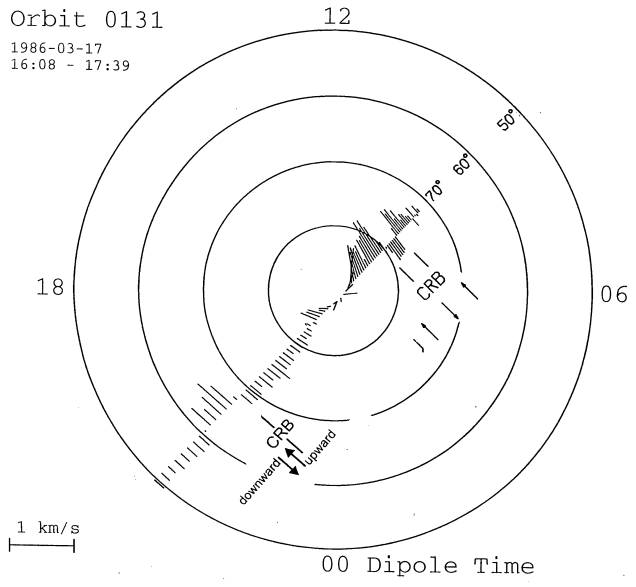

Fig. 8. Viking convection velocity mapped to the ionosphere in the corotating frame, based on the spin plane component of the electric field for the pass shown in Figure 1. Averaging interval is 60 seconds. The convection reversal boundaries (CRB) and FAC directions are marked.

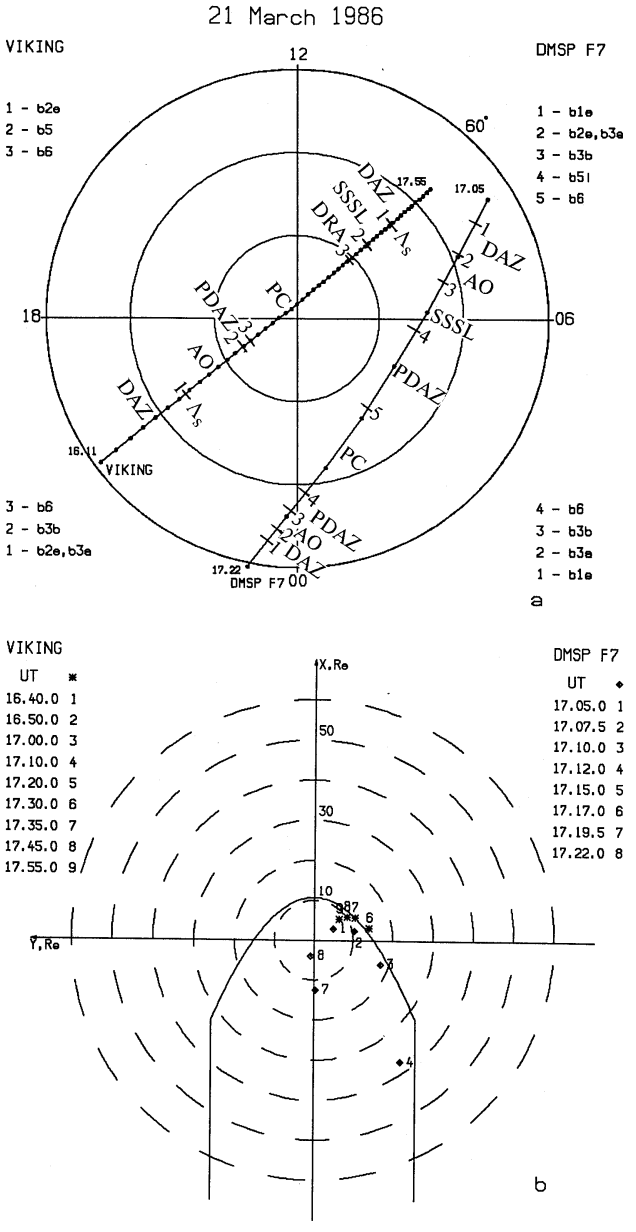

Fig. 9. The same as Fig. 1 except for the trajectories on 21 March 1986.

regime (Region 2) and the DRA regime (Region 0, which is located poleward of the Region 1 and in which FACs are controlled by the IMF component B_y). According to the electric field measurements, antisunward convection is observed between 1715 UT and 1720 UT, with sunward convetion both before and after this interval. Antisunward convection prevails in the SSSL regime, whereas the AO and DAZ regimes are located in regions with sunward convection.

The direction and velocity of the plasma convection at ionospheric altitudes perpendicular to the magnetic field and to the satellite's velocity direction are shown in Fig. 8, where the boundaries associated with changes in convection direction are marked. Arrows again show the FAC direction. In the dawn sector, the convection velocity increases with latitude and the convection direction is sunward up to $\Phi \sim 78°$ (in the DAZ and the AO). Then the convection direction changes to antisunward and remains so throughout most of the SSSL regime (up to $\Phi \sim 80°$). A new convection reversal is connected with the DRA regime, where the convection direction, as well as the FAC direction, are controlled by the IMF azimuthal component B_y. The sunward convection points to a negative B_y. In the dusk sector, the convection reversal boundary (CRB) is close to the poleward boundary of the region with FAC. The convection is sunward in the DAZ region (downward FAC) and throughout most of the AO regime (upward FAC).

2.2.2 Example 2: 21 March 1986

Figure 9a shows the DMSP F7 and Viking trajectories in the polar projection and Fig. 9b shows the projection of these trajectories to the magnetosphere equatorial plane. The notations in these figures are the same as in Fig. 1a,b. It is only possible to map to the equatorial plane the prenoon Viking trajectory portion (after 1640 UT), for which there is IMF data.

During 1600–1800 UT, hourly average values of the IMF components are -1.3 nT and 0.3 nT for B_z, 6.5 nT and 6.0 nT for B_y; hourly average values of the solar wind V are 519 km/s and 506 km/s, and for the density n, they are 5.0 cm^{-3} and 4.8 cm^{-3}. This time interval encompasses the final period of an intensive substorm and the beginning of a new one, starting at 1630 UT (AU is 46 nT and 60 nT, AL is -45 nT and -142 nT, AE is 92 nT and 204 nT, Kp is 3, Dst is

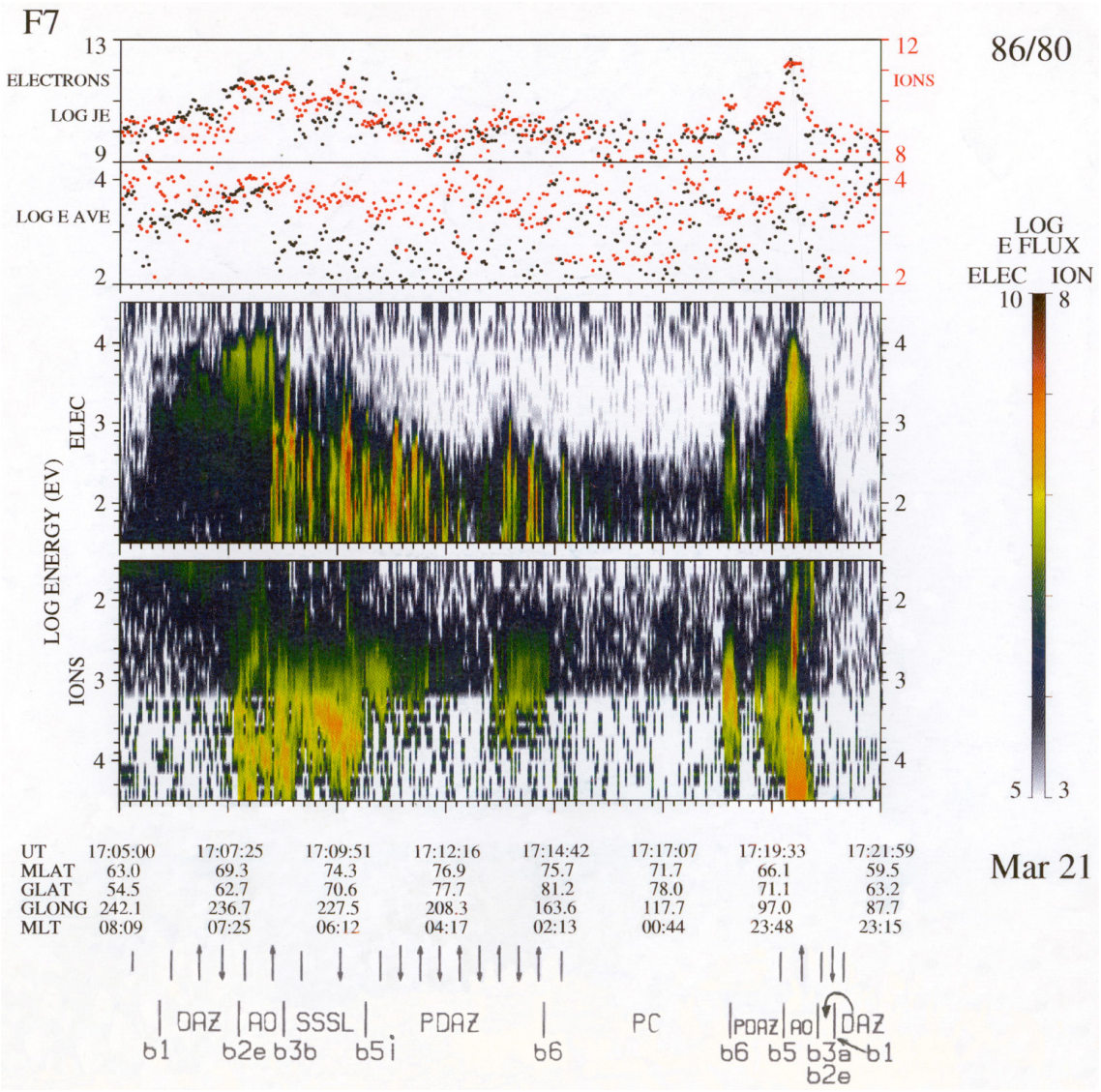

Fig. 10. The same as Fig. 2, except for the spectrogram on 21 March 1986, 1705–1722 UT.

−33 nT and −37 nT).

The DMSP F7 particle spectrogram is shown in Fig. 10. On the whole, the particle precipitation regimes are the same as for the DMSP pass on 17 March, in Fig. 2. The auroral plasma is seen for the first time at 1705:40 UT (*b*1*e* boundary) at $\Phi = 64.6°$ and 8.0 MLT. The diffuse precipitation of electrons with energy up to 10 keV, and with ion precipitation below threshold is measured until 1707:25 UT (the *b*2*e* and *b*3*a* boundaries with $\Phi = 69.3°$ and 7.4 MLT); between *b*1*e* and *b*2*e* is the DAZ regime. The regime with structured electron precipitation of energy up to 20 keV and very intensive fluxes of energetic ions (the AO regime) is located at higher latitudes between the *b*3*a* and *b*3*b* boundaries (1708:20 UT, $\Phi = 71.2°$ and 7.1 MLT). At the *b*3*b* boundary, the electron spectra become sharply soft, the fluxes are structured with an average energy at about 300 eV, and ions with several keV are observed. This region with the poleward boundary *b*5*i* (1710:20 UT, $\Phi = 74.8°$ and 5.8 MLT) is the SSSL regime. During traversal of this region, the electron and ion energies sharply decrease. The satellite trajectory between 1708:20 and 1710:20 UT can be mapped close to the magnetopause (the LLBL region). Before the satellite enters into the polar cap (*b*6 boundary at 1714:28 UT, $\Phi = 75.8°$ and 02.4 MLT) very soft structured electron precipitation and diffuse ion precipitation is observed (PDAZ). Close to the polar cap boundary the precipitating particle fluxes increase, which may be caused by a weak auroral arc located at the polar cap boundary. This precipitation regime is mapped to the magnetospheric tail at geocentric distances of about 30–60 R_e.

In the near midnight sector, the satellite sequentially intersects the boundaries *b*6 (1718:27 UT, $\Phi = 68.9°$ and 0.2 MLT), *b*3*b* (1719:33 UT, $\Phi = 66.1°$ and 23.8 MLT), *b*3*a* (1720:02 UT, $\Phi = 64.9°$ and 23.7 MLT), and *b*1*e* (1720:46 UT, $\Phi = 63.5°$ and 23.6 MLT). All of these boundaries are

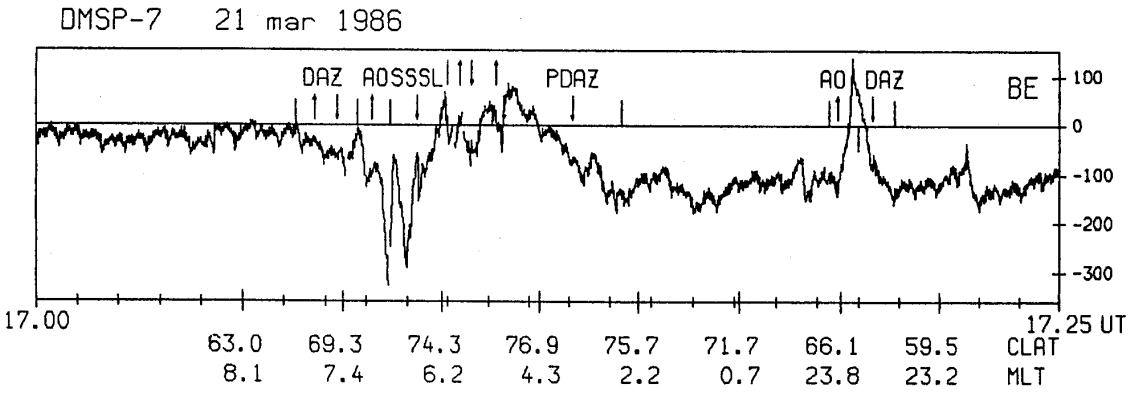

Fig. 11. The same as Fig. 4, except for 21 March 1986, 1700–1725 UT.

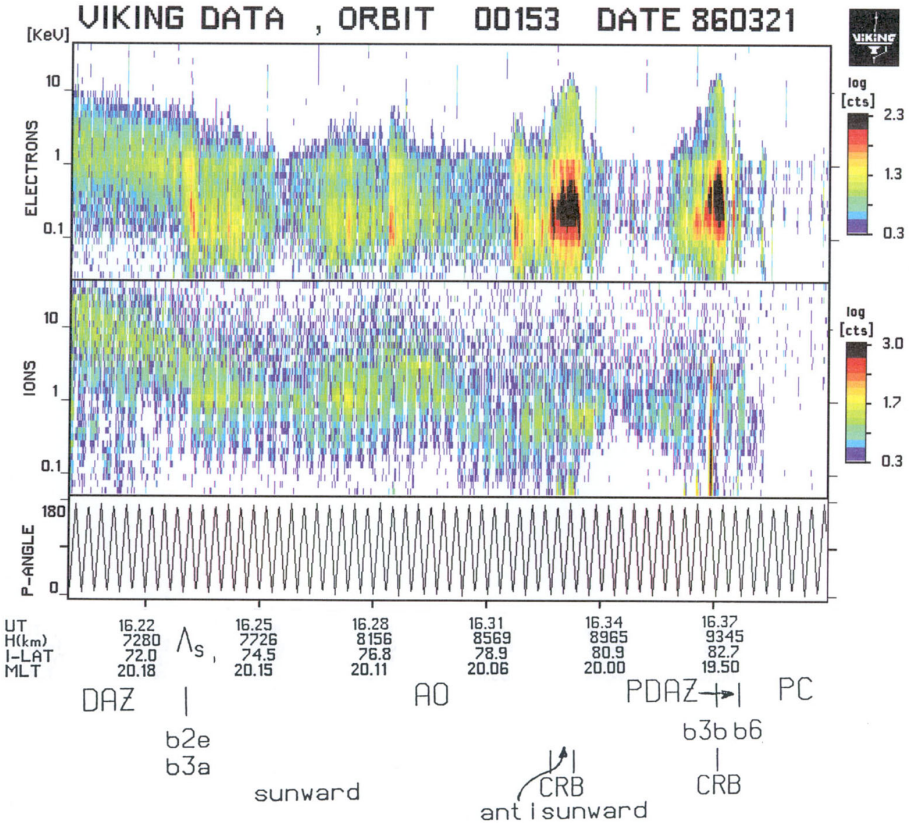

Fig. 12a. The same as Fig. 5a, except for orbit 153 on 21 March 1986, 1620–1736 UT.

mapped to the nightside magnetosphere at geocentric distances of 10–40 R_e in the equatorial plane and separate the regimes marked in Fig. 9a as PDAZ, AO, and DAZ.

The precipitating electron and ion spectra in the different regimes encountered by DMSP F7 show:

a) in the DAZ, hard electrons with energy more than 0.3 keV are measured in the dawn sector. Ion fluxes are below threshold, but hard ions, softer electrons and essentially no hard electrons are observed in the midnight sector;

b) in the AO regime, keV electrons dominate. High fluxes of energetic ions are seen in the midnight sector, one order of magnitude lower fluxes in the dawn sector;

c) in the SSSL regime, electrons with energy of several hundred eV and keV ions dominate;

d) in the BAL regime, the electron spectra indicate the presence of field-aligned acceleration. The sharp differences in the energy fluxes of ions with energy of more than 5 keV between the SSSL and BAL regimes is an additional argument, showing that both these regions are needed and that they correspond to different magnetospheric domains.

The variation of the east-west magnetic field component along the DMSP F7 passes, presented in Fig. 11, reveals

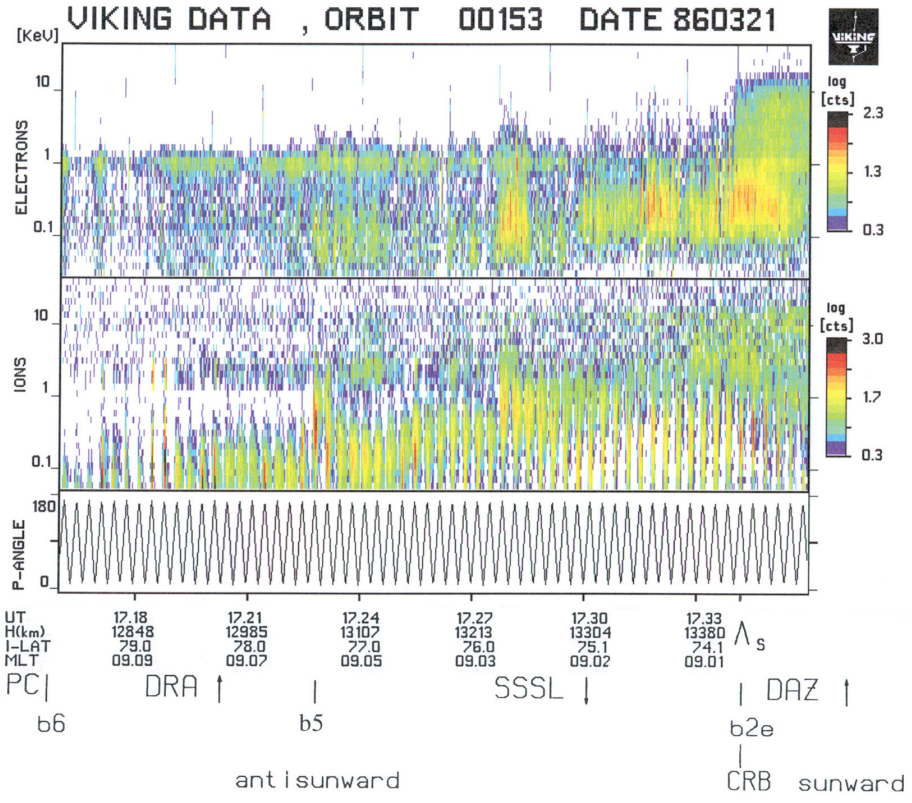

Fig. 12b. The same as Fig. 5b, except for orbit 153 on 21 March 1986, 1620–1736 UT.

a complicated dayside system of field-aligned currents and a rather simple near midnight system. In the near midnight sector, the large-scale FAC flows into the ionosphere in the DAZ regime and flows out in the AO regime. In the morning, FAC flows into the ionosphere in the SSSL regime and flows out in the AO regime. In addition to this main intensive FAC pair in the dawn sector, the magnetic field variations suggest multiple small scale current structures or rapid temporal variations in the DAZ, SSSL, and PDAZ regime. This is associated with strongly structured precipitating particle fluxes, indicating an inhomogeneous ionospheric conductivity structure.

The Viking satellite (orbit 153) traverses the high-latitude region in the dusk and prenoon sectors, with a cut also through the polar cap. Figure 9a shows the Viking trajectory and plasma regime boundaries; Fig. 12a,b shows the Viking particle spectrograms.

In the dusk sector at 1623:20 UT ($\Phi = 73.2°$ and 20.3 MLT), Viking crosses the boundary *b*3*a* which is identified by the most equatorward intensive auroral arc location. The plasma regime equatorward of *b*3*a* is characterized by the presence of energetic ions with energy up to some ten keV, isotropic pitch-angle distributions in the upper hemisphere and the absence of upward moving ions. At 1623:20 UT, the flux of electrons with energies of several tens of keV decreases by an order of magnitude at all pitch-angles. This means that the boundary *b*3*a* is simultaneously the boundary (Λ_s) of the stable trapping energetic electrons, which in the nightside sector separates the inner magnetosphere from the plasma sheet (Ackerson and Frank, 1972).

Correspondingly, the plasma regime equatorward of Λ_s is the DAZ and poleward of it, the AO. Within the AO, intensive electron precipitation is connected with discrete auroral forms. Poleward of the high-latitude discrete forms is the poleward boundary of AO (*b*3*b*, 1636 UT, $\Phi = 82.7°$ and 19.8 MLT); the narrow belt of soft electron precipitation (PDAZ) separates the AO from the polar cap (PC). The boundary *b*6 is crossed by the satellite at 1637:20 UT ($\Phi = 82.9°$ and 19.7 MLT).

In the prenoon sector, after crossing of the polar cap boundary *b*6 (1716 UT, $\Phi = 80°$ and 9.6 MLT), the satellite enters into the plasma regime with diffuse precipitation of soft (< 1 keV) electrons and very soft (< 0.3 keV) upflowing ion beams. The ion energy increases when the satellite goes deeper into the layer. This behaviour is typical for the DRA regime. Its boundary *b*5 is intersected by the satellite at 1723 UT ($\Phi = 77.4°$ and 9.1 MLT), when structured electron precipitation and upward ions beams are observed, first at low energies up to 0.5 keV, and then at energies up to 1 keV. This plasma SSSL regime is mapped to the magnetopause region and it is naturally connected with the LLBL. Below, it will be shown that the convection results agree with such an interpretation. The equatorial boundary of the SSSL (1734 UT, $\Phi = 73.8°$ and 09 MLT) coincides with a sharp increase in the fluxes of precipitating electrons with energies of about 10 keV, and with the stable trapping boundary (Λ_s) of electrons, with energies of several tens of keV. At lower latitudes

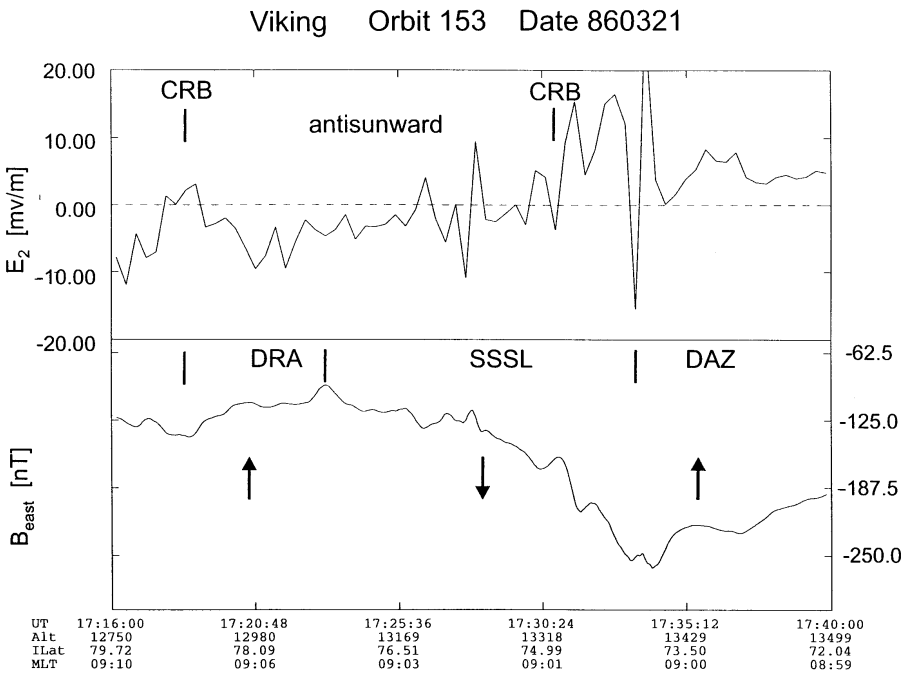

Fig. 13. The same as Fig. 7b, except for 21 March 1986, 1715–1740 UT.

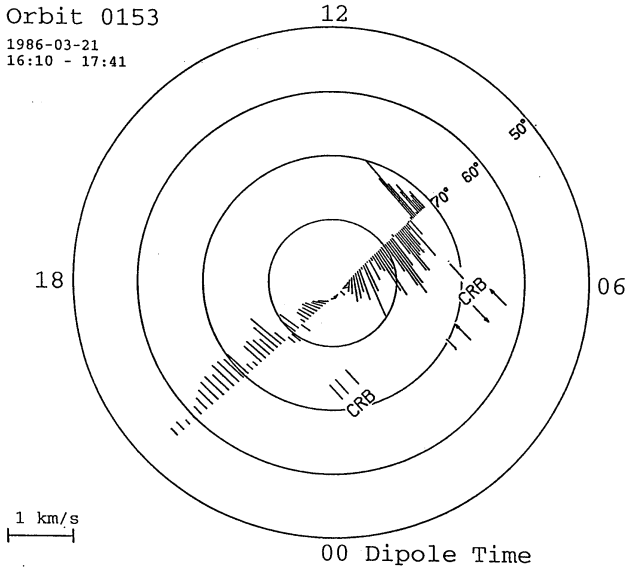

Fig. 14. The same as Fig. 8, except for 21 March 1986, 1610–1741 UT.

the plasma regime is typical for the DAZ in the dawn sector; there is diffuse electron precipitation with energy increasing and anisotropic ion pitch-angles distributions. As we will see, this plasma regime is associated with sunward convection and the existence of upward FACs at these latitudes. It should be noted that on this pass through the prenoon sector, there is no regime which can be identified as the AO regime.

The variations of the east-west magnetic field component and the E2 component of the electric field measured by Viking is shown in Fig. 13. As in the previous case, the electric field measurements can be used to reliably deduce the dominant direction of the convection. Only data from the prenoon sector is available. The geomagnetic field variations show the existence of three FAC sheets: current inflow into the ionosphere in the SSSL regime, and outflow in the DRA and DAZ regimes. Electric field measurements show that the DRA regime and most of the SSSL regime are located in a region with antisunward convection. The whole DAZ regime and the equatorward part of the SSSL regime are located in a sunward convection region. The convection pattern, as observed by Viking in the prenoon sector, is shown in Fig. 14. Typical sunward convection is seen in the DAZ regime and antisunward convection is seen over the whole latitude range poleward of *b2e* (Λ_s). These latitudes occupy most of the SSSL and DRA regimes. During Viking orbit 131 (Fig. 8), the convection was sunward in the DRA regime. The reason for the difference in the convection direction is the close connection with the interplanetary magnetic field orientation. In the dusk sector the convection is sunward during practically the whole time it takes to cross the auroral precipitation region. Several short convection reversals in the AO regime may be associated with auroral arcs in this region.

3 Plasma regime boundaries, field-aligned currents and convection in the dawn sector

It seems reasonable to include more cases of dawn sector traversals, such as the two cases described in detail above. Viking measurements from March to May 1986 were analyzed and passes for which there were simultaneous measurements of plasma and the magnetic and electric fields, as well as measurements of the interplanetary medium were chosen. Furthermore, DMSP observations for the same time intervals were included. For these passes, the boundaries of the

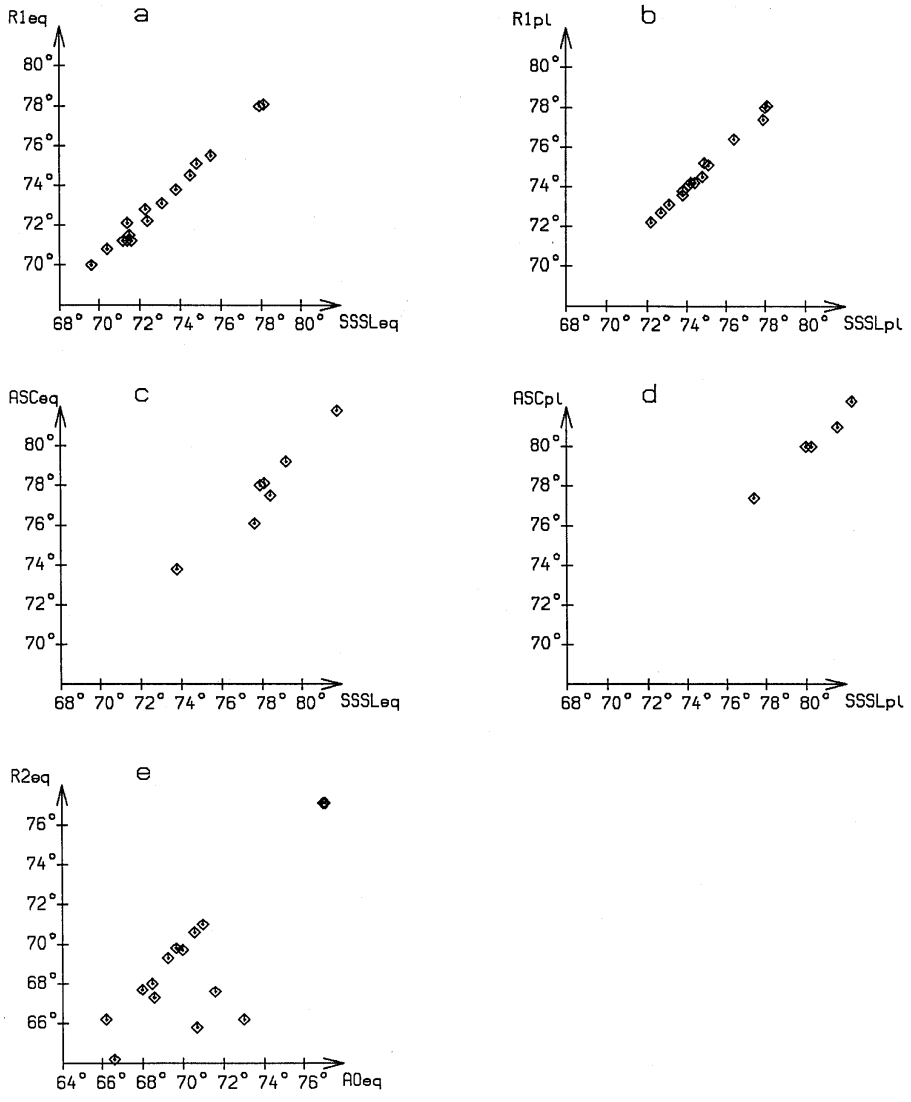

Fig. 15. Comparison of the location of plasma regime boundaries, field-aligned currents and convection reversals in the dawn sector, based on the DMSP and Viking observations: **(a)** $SSSL_{eq}$ and $R1_{eq}$; **(b)** $SSSL_{pl}$ and $R1_{pl}$; **(c)** $SSSL_{eq}$ and ASC_{eq}; **(d)** $SSSL_{pl}$ and ASC_{pl}; **(e)** AO_{eq} and $R2_{eq}$.

plasma regions, the boundaries of inflowing and outflowing field-aligned currents and the CRB location were identified. Figure 15 shows a summary of the obtained relations. The boundaries in the corrected geomagnetic latitudes vary over rather wide ranges, according to the disturbance level and MLT for the individual traversals during the interval from 0400 to 1000 MLT.

Figure 15a shows equatorward boundaries of the R1 field-aligned currents and the SSSL regime. Figure 15b compares the poleward boundaries of the same regions. The close coincidence of the boundaries testifies that the downward FAC are located within the SSSL regime, over the whole MLT interval and for all disturbance levels. The average values of the corrected geomagnetic latitudes of the SSSL regime for 0700 MLT are $SSSL_{eq} \approx 73°$ and $SSSL_{pl} \approx 76°$. The CRB, which separates the AO sunward convection from the SSSL anti-sunward convection, practically always coincides with $SSSL_{eq}$ (Fig. 15c). The poleward SSSL boundary is often clearly associated with a convection reversal (those cases are shown in Fig. 15d). However, sometimes the anti-sunward convection extends further poleward out of the SSSL regime, covering also the DRA regime. Thus, for most of the SSSL regime, the convection is anti-sunward in all cases under investigation, but the anti-sunward convection may extend to the region poleward of SSSL. There were two cases with such a wide dayside anti-sunward convection region; these were the only cases for which the IMF azimuthal component, B_y, was positive. This means that the convection in the poleward portion of the auroral luminosity region is controlled by the IMF B_y component. Therefore, in these cases, the poleward boundary of anti-sunward convection is located poleward of $SSSL_{pl}$.

The upward FACs (R2 region) primarily embrace the auroral oval latitudes. The R2 current adjoins the equatorward portion of the R1 current in a similar way as the AO regime adjoins the SSSL regime. Therefore the poleward boundary of R2 currents approximately coincides with the auroral oval poleward boundary. The equatorward boundary of these

currents ($R2_{eq}$) approximately coincides with AO_{eq} in most cases (Fig. 15e). In 10 out of 14 cases, these boundaries coincide with each other within $\pm 0.2°$ and only in 4 cases, the difference reaches 2°–7°. For these latter cases, $R2_{eq}$ coincides with the equatorial boundary of the diffuse precipitation region. Thus, in the dawn sector in most cases, the R2 FACs are located at auroral oval latitudes, but sometimes also embrace the diffuse luminosity region equatorward of the oval.

In case of the evening and night intersections of the auroral region by the satellites, our results agree with those described in literature and, therefore, they are not shown explicitly. The equatorial and poleward boundaries of Region 1 FACs approximately coincide with the corresponding boundaries of the AO regime. Thus, Region 1 FACs in the dawn and dusk MLT sectors are connected with substantially different plasma regimes, i.e. SSSL in the dawn sector and AO in the dusk sector.

4 Summary and discussion

The observational results are summarized in Fig. 16. They are typical for quiet and weakly disturbed conditions. Figure 16 (upper panel) shows schematically particle patterns for the precipitating electrons and ions. The corrected geomagnetic latitudes and energy intervals of the various regimes correspond to 0700 MLT. Figure 16 (lower panel) shows the boundaries of the particle precipitation regions mapped into the magnetospheric equatorial plane.

Magnetic field models may provide certain guidelines or constraints for mapping the various ionospheric plasma regimes to the magnetosphere. The mapping in Fig. 16 shows the location of particle precipitation regions, as defined in the polar ionosphere, and the possible source regions in the outer magnetosphere. For mapping, the paraboloidal model of the magnetospheric magnetic field by Alexeev et al. (1996) is used. The input model parameters correspond to the geomagnetic conditions in the weakly disturbed interval on 17 March 1986 at 1700 UT:

a) the ring current intensity on the Earth's surface is equal to -20 nT;

b) the geocentric distance to the subsolar point at the magnetopause is equal to 9.8 R_e;

c) the geocentric distance to the plasma sheet inner boundary at the midnight is equal to 7.3 R_e;

d) the magnetic flux in the magnetosphere tail lobes is 0.45×10^9 Wb. It corresponds to an open-closed field lines boundary, which is located in the noon sector at 80.0° and in the midnight sector at 68.3°;

e) the solar wind dynamic pressure is equal to 4.56 nP.

The observations can be summarized as follows: the DAZ regime is characterized by energetic electron precipitations and the absence of precipitations of auroral energy ions. This region is the outer radiation belt and indeed, the DAZ regime is mapped to the inner magnetosphere. Since the auroral electron energies in the DAZ are substantially less than the particle energies in the radiation belts, it is necessary to identify this plasma regime by its own name. Feldstein and Galperin (1985) suggested the notation Remnant Layer, as the RL auroral plasma is the remnant of plasma from the central plasma sheet, entering the RL by convection and injection.

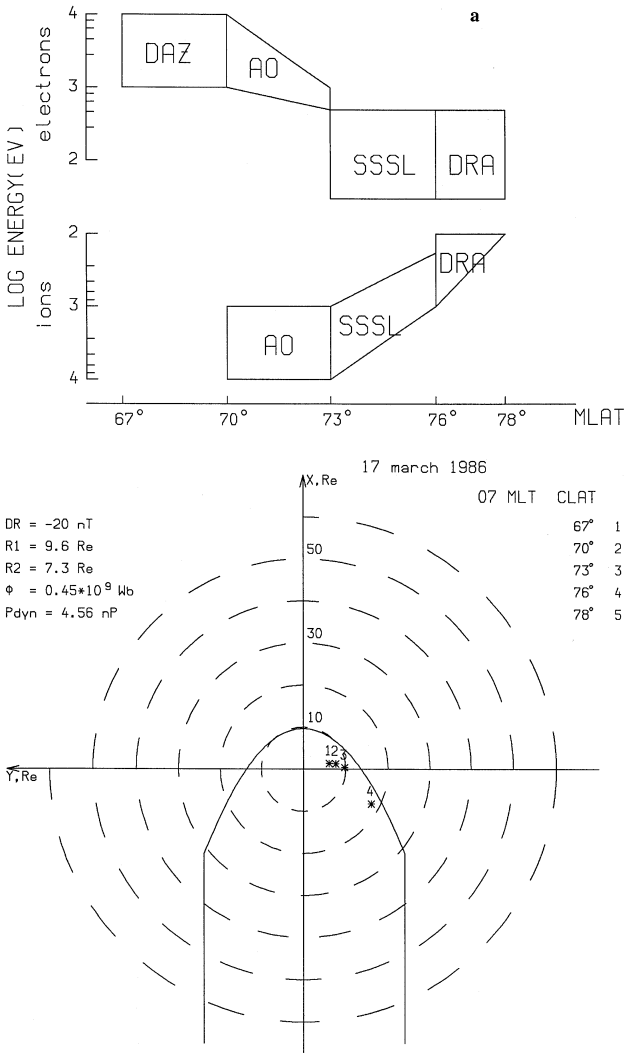

Fig. 16. Sketches showing the location of various particle precipitation regimes in the dawn high-latitude region (upper panel) and corresponding plasma regime boundaries mapped to the outer magnetospheric equatorial plane (lower panel).

As the electrons drift in the dawn-dusk electric field, their energy increases (Torkar et al., 1985). This allows one to explain the disappearance of the typical near-midnight effect of electron energy increase with latitude. Since during the azimuthal drift, electrons gain energy, which considerably exceeds their initial one, the energy dependence on radial distance is smoothed out in the RL on the dawn sector.

The absence of ion precipitation in the dawn RL is apparently connected with a change in the pitch-angle distribution of ions moving from the nightside through dusk, and noon towards dawn (Sauvaud et al., 1998). Up to the morning sector, ions moving around the Earth are mainly trapped, with

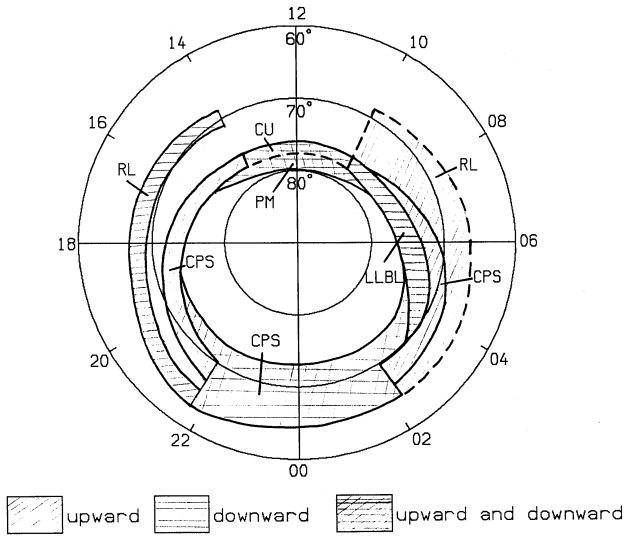

Fig. 17. Spatial distribution of downward/upward FACs in geomagnetic latitude–local geomagnetic time coordinates. Plasma domains in the magnetosphere connected by magnetic field lines with the corresponding ionospheric FAC regions are marked.

their pitch-angle distributions at a peak near 90°. The maximum of the precipitating ion flux is observed in the RL at dusk (Newell et al., 1996).

The AO regime represents the continuation of the structured electron precipitation region to the dawn sector. Its projection mapped to the magnetosphere is located inside the magnetosphere, but relatively close to the magnetopause. Its sunward side is the extension of the nightside central plasma sheet, past the dawn/dusk flanks. During the transition from the nightside sector to the dayside sector, the equatorial cross section of CPS decreases to $\sim 1R_e$ at 0700 MLT. The CPS is virtually absent at the $\sim$ 1000 MLT meridian. In the AO, the electron energy first decreases smoothly, with latitude (corresponding to the approaching of the magnetopause), then it jumps at the boundary between AO and SSSL regimes. The AO electron energy of several keV is typical for CPS.

The behaviour of the electron and proton luminosity, known for a long time from literature, may be explained by the difference in the ion energy spectra and pitch-angle distributions existing in the DAZ and AO plasma regimes at dusk and dawn sectors. According to Evlashin and Evlashina (1981), the proton luminosity is located equatorward of the electron discrete forms in the dusk sector and poleward of them in the dawn sector. Indeed, in the dusk sector, the ion precipitation occurs at the DAZ latitudes, equatorward of the AO. This leads to the proton luminosity's location equatorward of the auroral discrete forms. In the dawn sector, there is no ion precipitation in the DAZ. Such precipitation is observed in the AO and poleward of it. This fact causes the difference in the mutual location of the electron and proton aurorae in both sectors.

The SSSL regime is characterized by fluxes of soft structured electrons and low-energy ions. It is mapped close to the magnetopause, i.e. to the low-latitude boundary layer (LLBL). The SSSL ion spectra closely resemble those observed *in situ* in the LLBL (Haerendel et al., 1978; Traver et al., 1991).

The DRA regime is located poleward of the SSSL and very soft electron precipitation is observed there. According to magnetic field line tracing, this auroral precipitation type is located on open field lines, because its magnetic field line projections do not intersect the magnetospheric equatorial plane. Such high-latitude precipitation with ion energies decreasing with latitude are naturally connected with the Plasma Mantle (PM) on the magnetospheric tail surface. The DRA ion spectrum is similar to the de-energized magnetosheath ions in the PM.

The mapping scheme of plasma regimes from auroral altitudes at dawn to the magnetospheric plasma domains during low-level magnetic activity is summarized in Table 1, which also shows the corresponding characteristics of the plasma regimes and associated FAC and magnetospheric convection directions.

The scheme of the spatial distribution of large-scale field-aligned currents is shown in Fig. 17. The inflowing and outflowing FACs are shown by different hatching. The regions where FACs may change their directions, according to the IMF orientation (the mantle and the near-noon auroral oval sector) or the disturbance level (the auroral oval near-midnight sector), are marked by double hatching.

It should be specifically emphasized that the Region 1 FAC in the dawn and evening sectors are generated in absolutely different plasma domains of the distant magnetosphere: in the evening sector, they are associated with the CPS, which maps to the discrete auroral form region (AO regime) at ionospheric altitudes, and at dawn, they are connected to the LLBL, which maps to the ionospheric soft structured precipitation region (SSSL regime). This means that FACs at evening and dawn, which are traditionally combined into one single Region 1 current system, are really generated in different magnetospheric regions. Apparently, their continuous existence is caused by permanently available processes in these magnetospheric regions. They are related only by the common circumstance that the reason for the Region 1 FAC existence in the different time sectors is the solar wind plasma interaction with the geomagnetic field.

The field-aligned currents in Region 2 may also be generated in different magnetospheric plasma domains: in the dusk sector in the RL, in the dawn sector in the CPS (more common) or, alternatively, in the wide region covering CPS and RL (rarer). Thus, FACs of Region 2, similar to the FACs Region 1, may be generated in different magnetospheric plasma domains.

Upward FAC of Region 0 have been originally referred to as cusp currents (Iijima and Potemra, 1976). Analysis of geomagnetic field variations on the Earth's surface at high latitudes, combined with different sources for the field variations and subsequent calculation of the spatial FACs distribution (IZMEM model) have shown (Levitin et al., 1982) that:

a) the Region 0 FAC is located in the day sector, partly

Table 1. Characterization, boundaries and mapping at the dawn sector precipitation regions to magnetospheric plasma domains

AURORAL ALTITUDES	MAGNETOSPHERIC PLASMA DOMAINS
$b1$ – equatorward boundary of diffuse auroral precipitation	Plasmapause
DIFFUSE AURORAL ZONE – DAZ	REMNANT LAYER – RL
Weak luminosity, diffuse high-energy electron precipitation (E up to 10 keV, flux peak $\sim 10^7$ eV(cm^2 s sr eV)$^{-1}$), no ion precipitation at these energies, upward FACs (Region 2) are sporadically present, sunward convection	Region within the Outer Radiation Belt (ORB), trapped ions dominate, plasma moves from the plasma sheet
$b2$ – poleward boundary of diffuse auroral precipitation	Inner boundary of plasma sheet
AURORAL OVAL – AO	CENTRAL PLASMA SHEET – CPS
$b3a$ – equatorward boundary of structured precipitation (auroral oval)	Earthward boundary region of central plasma sheet
Precipitation of electrons with energies of several keV and ions up to 10 keV (flux peak $\sim 5 \times 10^7$ eV (cm^2 s sr eV)$^{-1}$ for electrons and 10^6 eV (cm^2 s sr eV)$^{-1}$ for ions); electron bursts below 1 keV, intensive upward moving ion beams with $E < 1$ keV, background isotropic ion distribution with energies of several keV; weaker intensity of auroral forms compared to arcs in the dusk and nightside sectors; upward FACs (Region 2); sunward convection	The narrow region in the magnetoshpere between the ORB and the boundary layer on the magnetopause. The CPS radial extent decreases from the nightside to the prenoon sector
$b3b$ – poleward boundary of high-energy structured electron precipitation	Outer boundary region of central plasma sheet, inner boundary of LLBL
SOFT SMALL-SCALE LUMINOSITY – SSSL	LOW-LATITUDE BOUNDARY LAYER – LLBL
Small-scale precipitations of electrons with $E \sim 0.2$ keV and ions with $E \sim 1$ keV, with flux peak $\sim 5 \times 10^8$ eV (cm^2 s sr eV)$^{-1}$ for electrons and $\sim 5 \times 10^6$ eV (cm^2 s sr eV)$^{-1}$ for ions; auroral structured luminosity; essentially isotropic populations, except for separate upward moving ionic beams with $E < 1$ keV; downward FACs (Region 1); anti-sunward convection	The plasma layer close to the magnetospheric boundary with closed magnetic field lines; plasma beams
$b5$ – poleward boundary of region with small scale structured electron precipitation, sharp decrease of ion energy	Outer boundary of LLBL
DIFFUSE RED AURORA – DRA	PLASMA MANTLE – PM
Weak diffuse 630 nm emission; anisotropic fluxes of very soft electrons and ions with empty upward loss cone and flux peak $\sim 10^6$ eV (cm^2 s sr eV)$^{-1}$; ion beams; directions of the convection and FACs are controlled by the IMF azimuthal component	The plasma layer located outside of the magnetopause; de-energized magnetosheath plasma; open magnetic field lines
$b8$ – poleward boundary of diffuse red aurora in near-noon region	Boundary of plasma mantle in the tail lobe
$b6$ – poleward boundary of auroral precipitation (boundary of polar cap)	Boundary of tail lobe
POLAR CAP – PC	TAIL LOBES – TL
Very weak luminosity and low energy particles precipitation (polar rain)	Extremly low plasma density. Open magnetic field lines
$b7$ – equatorward boundary of very soft precipitation near the poleward edge of auroral region in night sector	Inner boundary of low energetic electron layer (LEL) between PS and TL

within the Region 1 extension towards noon and partly within the the polar cap, i.e. poleward of the Region 1 current;

b) the intensity and direction of Region 0 FAC is controlled by the IMF component B_y;

c) the existence of such currents made it possible to explain cases of anomalous FAC direction distributions in the poleward region (McDiarmid et al., 1977; Levitin et al., 1982) with a reverse polarity of Region 1 and Region 2 at high latitudes.

Later, the FAC Region 0 connection with the IMF B_y component and their location at plasma mantle latitudes were demonstrated *in situ* by satellite observations (Bythrow et al., 1988; Erlandson et al., 1988; de la Beaujardiere et al., 1993).

The specific Circumpolar Ion Precipitation regime (CPIP), suggested first by Nishida et al. (1992, 1993), is located in the dawn sector on the poleward side of the Transition

Boundary (TB), which is proposed as the plasma sheet boundary and identified by a sharp decrease in the energetic electron flux. Yet poleward of this boundary, the DMSP and Viking satellites observed not only intensive ion fluxes, but also intensive fluxes of auroral energy electrons as well. A detailed analysis of DMSP satellite data by Troshichev and Nishida (1992) showed that the TB really separates the high-energy electron region from the softer electron and ion precipitation region located further poleward. According to the above suggested classification, it is the boundary *b3b* between the AO and the SSSL where the auroral electron spectrum sharply softens. In reality, the spectrograms of all the DMSP satellite passes intersecting the dawn sector which have been presented in Troshichev and Nishida (1992) agree with this interpretation. According to this interpretation, the CPIP regime is nothing more than the SSSL regime. At these latitudes, there are not only ion fluxes, but electron fluxes too. A more detailed discussion of this problem is contained in Newell and Meng (1994b) and Nishida and Mukai (1994).

Acknowledgements. The Viking Project was managed and operated by the Swedish Space Corporation under contract from the Swedish Board for Space Activities. This work was supported by grant INTAS-RFBR-95-0932 and by the Russian Foundation of Basic Researches project codes 99-05-65611 and by the ISSI, Bern.

The Editor in Chief thanks R. Fujii and T. Iijima for their help in evaluating this paper.

References

Ackerson, K. L. and Frank, L. A., Correlated satellite measurements of low-energy electron precipitation and ground-based observations of a visible auroral arc, J. Geophys. Res., 77, 1128–1136, 1972.

Akasofu, S. I., Recent progress in studies of DMSP auroral photographs, Space Sci. Review, 19, 169–215, 1976.

Alexeev, I. I., Belenkaya, E. S., Kalegaev, V. V., Feldstein, Ya. I., and Grafe, A., Magnetic storms and magnetotail currents, J. Geophys. Res., 101, 7737–7747, 1996.

Block, L. P., Falthammar, C.-G., Lindqvist, P.-A., Marklund, G. T., Mozer, F. S., and Pedersen, A., Measurement of quasistatic and low frequency electric fields on the Viking satellite, Rep. TRITA-EPP-87-02, Royal Inst. Tech., Stockholm, 1987.

Bythrow, P. F., Potemra, P. A., Erlandson, R. E., Zanetti, L. J., and Klumpar, D. M., Birkeland currents and charged particles in the high-latitude prenoon region: a new interpretation, J. Geophys. Res., 93, 9791–9803, 1988.

Craven, J. D. and Frank, L. A., Diagnosis of auroral dynamics using global auroral imaging with emphasis on large-scale evolutions, in Auroral Physics, Cambridge UP, Eds. C.-I. Meng, M. J. Rycroft, and L. A. Frank, Cambridge UP, 273–288, 1991.

de la Beaujardiere, O., Watermann, J., Newell, P., and Rich, F., Relationship between Birkeland current regions, particle precipitation, and electric fields, J. Geophys. Res., 98, 7711–7720, 1993.

Eastman, T. E., Frank, L. A. and Huang, C. Y., The boundary layers as the primary transport regions of the Earth's magnetotail, J. Geophys. Res., 90, 9541–9560, 1985.

Erlandson, R. E., Zanetti, L. J., Potemra, P. A., Bythrow, P. F., and Lundin, R., IMF B_y dependence of region 1 Birkeland currents near noon, J. Geophys. Res., 93, 9804–9814, 1988.

Evlashin, L. S. and Evlashina, L. M., On the problem of the apstial-temporal distribution of auroral luminosity, in Aurora and airglow, N28, Publ. House Nauka, Moscow, 24–27, 1981.

Feldstein, Y. I. and Galperin, Y. I., The auroral precipitation regimes in the nightside magnetosphere sector, Cosmic Research, 34, N3, 227–247, 1996.

Frank, L. A., Plasmas in the Earth's magnetotail, Space Sci. Rev., 42, 211–240, 1985.

Galperin, Yu. I. and Feldstein, Ya. I., Mapping of the precipitation regions to the plasma sheet, J. Geomag. Geoelectr., 48, 857–875, 1996.

Haerendel, G., Paschman, G., Sckopke, N., Rosenbauer, H., and Hedgecock, P. C., The frontside boundary layer of the magnetosphere and the problem of reconnection, J. Geophys. Res., 83, 3295–3216, 1978.

Hardy, D. A., Schmitt, L. K., Gussenhoven, M. S., Marshall, F. J., Yeh, H.-C., Shumaker, T. E., Hube, A., and Pantazis, J., Precipitating electron and ion delectors (SSJ/4) for the block 5D/flights 6–10 DMSP satellites: Calibration and Data presentation, Rep. AFGL-R-84–0317, Air Force Geophys. Lab., Bedford, Mass., 1984.

Iijima, T. and Potemra, P. A., Field-aligned currents in the dayside cusp observed by Triad, J. Geophys. Res., 81, 5971–5979, 1976.

Iijima, T. and Potemra, T. A., Large-scale characteristics of field-aligned currents associated with substorm, J. Geophys. Res., 83, 599–615, 1978.

Kamide, Y. and Akasofu, S.–I., The location of the field-aligned currents with respect to discrete auroral arcs, J. Geophys. Res., 81, 3999–4003, 1976.

Levitin, A. E., Afonina, R. G., Belov, B. A., and Feldstein, Ya. I., Geomagnetic variations and field-aligned currents at northern high-latitudes and their relations to solar wind parameters, Phil. Trans. Roy. Soc, A304, 253–301, 1982.

McDiarmid, J. B., Budzinski, E. E., Wilson, M. D., and Burrows, J. R., Reverse polarity of field-aligned currents of high latitudes, J. Geophys. Res., 82, 1513–1519, 1977.

Newell, P., Burke, W. J., Sanchez, E. R., Meng, C.-I., Greenspan, M. E., and Clauer, C. R., The low-latitude boundary layer and the boundary plasma sheet at low altitude: prenoon precipitation regions and convection reversal boundaries, J. Geophys. Res., 96, 21013–21023, 1991a.

Newell, P. T., Burke, W. J., Meng, C.-I., Sanchez, E. R., and Greenspan, M. E., Identification and observations of the plasma mantle at low altitudes, J. Geophys. Res., 96, 35–45, 1991b.

Newell, P. T., Feldstein, Ya. I., Galperin, Yu. I. and Meng, C.-I., The morphology of nightside precipitation, J. Geophys. Res., 101, N5, 10737–10748, 1996.

Newell, P. T. and Meng, C.-I., Mapping the dayside ionosphere to the magnetosphere according to particle precipitation characteristics, Geophys. Res. Lett., 19, 609- 612, 1992.

Newell, P. T. and Meng, C.-I., Ionospheric projections of magnetospheric regions under low and high solar wind pressure conditions, J. Geophys. Res., 99, 273–286, 1994a.

Newell, P. T. and Meng, C.-I., Comment on "Unexpected features of the ion precipitation in the so-called cleft/low-latitude boundary layer region: association with sunward convection and occurance on open field lines" by A. Nishida, T. Mukai, H. Hayakawa, A. Matsuoka, K. Tsuruda, N. Kaya, and H. Fukunishi, J. Geophys. Res., 99, 19609–19614, 1994b.

Nishida, A. and Mukai, T., Reply to Comment on A. Nishida et al, J. Geophys. Res., 99, 23367–23370, 1994.

Nishida, A., Mukai, T., Hayakawa, H., Matsuoka, A., Tsuruda, K.,

Kaya, N., and Fukunishi, H., Unexpected features of the ion precipitation in the so-called cleft/LLBL region: association with sunward convection and occurrence on open field lines, J. Geophys. Res., 98, 11161–11176, 1993.

Nishida, A., Mukai, T., Tsuruda, K., and Hayakawa, H., Magnetospheric convection and current system in the dayside polar cap, in Proceedings of the 26th ESLAB Symposium – Study of the Solar-Terrestrial System, ESA SP-346, 183–192, 1992.

Nishida, A., Mukai, T., Yamamoto, T., Kokubun, S., and Maezawa, K., A unified model of the magnetotail convection in geomagnetically quiet and active times, J. Geophys. Res., 103, 4409–4418, 1998.

Nishida, A. and Ogino, T., Convection and reconnection in the Earth's magnetotail, in New perspectives of the Earth's magnetotail, 1997.

Potemra, T. A., Zanetti, L. J., Erlandson, R. E., Bythrow, P. F., Gustafsson, G., and Acuna, M. H., Observations of large-scale Birkeland currents with Viking, Geophys. Res. Lett., 14, 419–422, 1987.

Rich, F. J., Hardy, D. A., and Gussenhoven, M. S., Enhansed ionosphere-magnetosphere data from the DMSP satellites, EOS Trans. AGU, 66, 513, 1985.

Roelof, E. C. and Sibeck, D. G., The magnetopause shape as a bivariate function of IMF B_z and solar wind dynamic pressure, J. Geophys. Res., 98, 21421–21450, 1993.

Sandahl, I., Lundin, R. and Eliasson, L., The hot plasma spectrometers on Viking, KGI Tech. Rep., 035, Kiruna Geophysical Institute, Kiruna, Sweden, 1985.

Sandahl, I. and Lindqvist, P.-A., Electron populations above the nightside auroral oval during magnetic quiet times, Planet. Space Sci., 38, 1031–1049, 1990.

Sauvaud, J. A., Barthe, H., Aoustin, C., Thocaven, J. J., Rouzand, J., Penou, E., Popesku, D., Kovrazhkin, R. A., Afanasiev, K. G., The ion experiment on board the interball-Aurora satellite: Initial results on velosity-dispersed structures in the cleft and inside the auroral oval, Ann. Geophysicae, 16, N9, 1056-1069, 1998.

Torkar, K., Urban, A., Bjordal, J., Lundblad, J., Soraas, F., Smith, I., Dumbs, A., Grandal, B., Ulvick, J., and Vancour, R., Energy deposition rates by changed particles, J. Atmos. Terr. Phys., 47, 61–71, 1985.

Troshichev, O. A. and Nishida, A., Patterns of electron and ion precipitation in northern and southern polar regions for northward interplanetary magnetic field conditions, J. Geophys. Res., 97, 8337–8354, 1992.

Traver, D. P., Mitchell, D. G., Williams, D. J., Frank, L. A., and Huang, C.-Y., Particle observations during transversals of the low-latitude boundary layer, J. Geophys. Res., 96, 21025–21036, 1991.

Tsyganenko, N. A., Modeling the Earth's magnetospheric magnetic field confined within a realistic magnetopause, J. Geophys. Res., 100, 5599–5612, 1995.

Weiss, L. A., Reiff, P. H., Hilmer, R. V., Winningham, J. D., and Lu, G., Mapping the auroral oval into the magnetotail using Dynamics Explorer plasma data, J. Geomag. Geoelectr., 44, 1121–1144, 1992.

Winningham, J. D., Yasuhara, F., Akasofu, S.-I., and Heikkila, W. J., The latitudinal morphology of 10-ev to 10-kev electron fluxes during magnetically quiet and disturbed times in the 2100-0300 MLT sector, J. Geophys. Res., 80, 3148–3171, 1975.

Woch, J. and Lundin, R., The low-latitude boundary layer at mid-altitudes: identification based on Viking not plasma data, Geophys. Res. Lett., 20, 979–982, 1993.

Woch, J., Lundin, R., Potemra, T. A., and Shapshak, M., The projection of the magnetospheric boundary layers to mid-altitudes, in Physical signatures of magnetospheric boundary layer processes, Ed. J. A. Holtet and A. Egeland, Kluwer Academic Publ., 83–97, 1994.

Woch, J., Yamauchi, M., Lundin, R., Potemra, T. A., and Zanetti, L. J., The low-latitude boundary layer at mid-altitudes: relation to large-scale Birkeland currents, Geophys. Res. Lett., 20, 2251–2254, 1993.

Yamamoto, T., Kaneda, E., Hayakawa, H., Mukai, T., Matsuoka, A., Machida, S., Fukunishi, H., Kaya, N., Tsuruda, K., and Nishida, A., Meridional structures of electric potential relevant to premidnight discrete arcs: a case study from Akebono measurements, J. Geophys. Res., 98, 11135–11151, 1993.

Zmuda, A. J. and Armstrong, J. C., The diurnal variation of the region with vector magnetic field changes associated with fiald-aligned currents, J. Geophys. Res., 79, 2501–2512, 1974.